Results in Physics 52 (2023) 106786

Contents lists available at ScienceDirect

Results in Physics

journal homepage: www.elsevier.com/locate/rinp

Localized waves and their novel interaction solutions for a dimensionally reduced (2 + 1)-dimensional Kudryashov Sinelshchikov equation

Md. Nuruzzaman [a,b,*], Dipankar Kumar [a], Mustafa Inc [c,d,*], M. Alhaz Uddin [e], Rubayyi T. Alqahtani [f]

[a] Department of Mathematics, Bangabandhu Sheikh Mujibur Rahman Science and Technology University, Gopalganj 8100, Bangladesh
[b] Department of Textile Engineering, Uttara University, Dhaka 1230, Bangladesh
[c] Firat University, Science Faculty, Department of Mathematics, 23119 Elazig, Turkey
[d] Department of Medical Research, China Medical University, 40402 Taichung, Taiwan
[e] Department of Mathematics, Khulna University of Engineering & Technology, Khulna 9203, Bangladesh
[f] Department of Mathematics and Statistics, College of Science, Imam Mohammad Ibn Saud Islamic University, Riyadh, Saudi Arabia

ARTICLE INFO

Keywords:
Reduced (2+1)-dimensional Kudryashov-Sinelshchikov equation
Hirota bilinear method
Soliton solutions
Localized wave solutions
Interaction solutions

ABSTRACT

Propagation of the pressure waves in a liquid with gas bubbles is an important topic in the field of fluid dynamics and mathematical physics. The Kudryashov-Sinelshchikov equation is one of the models that describe the propagation of nonlinear waves in a bubbly liquid taking into consideration the viscosity of the liquid and the heat transfer. To explain such behaviors, we mainly focus in this study to explain the dynamics of localized waves and their variety of interaction solutions to a dimensionally reduced (2 + 1)-dimensional Kudryashov-Sinelshchikov equation with the aid of the Hirota bilinear method from *N*-soliton solutions. Four different forms of localized waves, including solitons, lumps, breathers, and rogues, are derived from the aforesaid equation based on the long wave limit approach. In particular, the localized waves can be used to find interaction solutions, which are the single breather or single lump formed by two solitons; interaction between one line soliton and one breather, as well as one line soliton and one lump soliton among the three solitons; interaction of the two-line soliton and one periodic breather, two periodic breathers, periodic breather and one lump soliton from the four solitons. The direction of propagation, phase shifts, shape, energy, and the variety of interaction solutions of localized waves are affected by these parameters. Moreover, analytical and graphical illustrations of these interaction solutions and their propagation properties are shown by the three-dimensional and density plots with the help of Maple 17. These newly discovered solutions in this study can be used to illustrate the interaction phenomenon of localized waves on ocean surfaces.

Introduction

The study of localized structures is a significant topic in the field of nonlinear science and mathematical physics. In nonlinear science, solitons, lump waves, breather waves, and rogue waves are localized structures that are useful in a variety of physical systems, including those that are described by the surface of the ocean, bubbling liquid gas, optical fiber, plasma, and other [1–4]. Considerably, these localized structures can also be seen on ocean surfaces when waves are propagated. Because of its important to nonlinear science, researchers have noticed to identify the localized structures of a class of nonlinear evolution equations (NLEEs). Conventionally, a solitary wave is a type of localized wave that exists in a confined area and does not change its shape as it moves forward at a steady speed [5]. On the other hand, soliton identity is preserved after pair-wise collisions [6]. However, a thorough investigation of such numerical simulations reveals that some nonlinear waves cannot be retrieved with their original identity after the collision. [7]. In these circumstances, a nonlinear evolution exact solution can permit the existence of solitons. Lumps, breathers, and rogues waves are also exact solutions that illustrate the localized behavior of any physical model. Lumps are solutions that decay rationally and are localized in all spatial directions solutions [8], on the other hand, breathers are solutions that have a periodic structure in one specific direction [9]. A rogue wave is a unique type of pattern that is localized in

* Corresponding authors.
E-mail addresses: nafizmath95@gmail.com (Md. Nuruzzaman), minc@firat.edu.tr (M. Inc).

https://doi.org/10.1016/j.rinp.2023.106786
Received 21 March 2023; Received in revised form 4 July 2023; Accepted 20 July 2023
Available online 28 July 2023

both space and time and is considered a rational solution [10]. Regarding the interest, researchers have investigated some new interaction solutions between four different kinds of nonlinear localized waves through NLEEs. Construction of analytic solutions for any nonlinear systems is challenging and time-consuming, but it is an important task for knowing the behavior of the system. Many popular and effective techniques [11–31] have been developed to construct analytic solutions for the variety of nonlinear systems by using symbolic software such as MATLAB, Maple, and Mathematica. Researchers [11–31] have demonstrated that the Hirota bilinear method (HBM) may be used to generate *N*-soliton solutions from any integrable NLEEs. Using the long wave limit technique with parameters, the localized solitons, lumps, breathers, rogues, and their variety of interaction solutions from *N*-soliton solutions have been found in a particular area of NLEEs [32–41].

In 2010, Kudryashov and Sinelshchikov [42] demonstrated the extensive application of nonlinear partial differential equations (PDEs) for describing pressure waves propagating within a mixture of gas bubbles and liquid. In this study, we consider the (3 + 1)-dimensional Kudryashov-Sinelshchikov (KS) equation [43], which leads to

$$(u_t + \alpha u u_x + \gamma u_{xxx})_x + d u_{yy} + e u_{zz} = 0, \tag{1.1}$$

where $u(x, y, z, t)$ is a function that denotes density, heat transfer, and viscosity; and α, γ, d, e are real constant parameters. Equation (1.1) explains the pressure waves in a mixture of gas bubbles and liquid by taking into account the viscosity of the heat transfer and liquid [44].

In the past, some scholars [45–56] studied and constructed some novel solutions to investigate (3 + 1)-dimensional KS equation. For instance, Feng et al., [45] obtained various rogue waves and resonant soliton solutions from the (3 + 1)-dimensional KS equation by using the Neural network method. Via the simplified linear superposition principle and velocity resonance together with the HBM, Kuo [46] investigated the multi-soliton solutions with resonance to the (3 + 1)-dimensional KS equation. With the aid of the Jacobi elliptic function method, Rehab et al., [47] constructed new solitary, shock wave, kink, and periodic wave solutions for the (3 + 1)-dimensional KS equation with in liquid gas. With the help of the unified and generalized unified methods, Jisha et al., [48] determined the rational traveling and traveling wave solutions to the KSE with variable coefficients. Hu et al., [49] constructed the nonautonomous lump solutions by using the HBM method from the (3 + 1)-dimensional KS equation in which the velocity and trajectory of these waves are observed with variable dispersion coefficients. By using the symmetry analysis, Yang et al., [50] obtained the symmetry reductions and geometric vector fields from the (3 + 1)-dimensional KS equation. Inc et al., [51] investigated the traveling and solitary wave solutions, which represent the singular-type, the king-type, and exponential solutions for the KS equation with the help of the Riccati Bernoulli sub-ODE method. Rehman et al., [52] used both the new extended hyperbolic function technique and the Sardar-subequation method for the KS equation that defines the behavior of nonlinear waves in gas–liquid mixtures. With the aid of a modified mathematical method, Seadawy et al., [53] determined the exact traveling and solitary wave solutions of the KS equation, their shape represents a dark, bright, singular, kink, and periodic wave, where applied various functions such as hyperbolic, trigonometric and elliptic functions. Akram et al., [54] constructed the traveling wave solutions for the KS equation by using the improved $\tan\left(\frac{\varphi(\eta)}{2}\right)$-expansion technique. Liu [55] explored the exact traveling wave solutions of the generalized KS equation with the aid of the auxiliary equation method.

It is important to notice here that Eq. (1.1) can be transformed with the help of the Korteweg-de Vries equation (KdV) [56], if we put $\alpha = 6$, $\gamma = 1, d = 0, e = 0, z = y$. Elsewhere, if we set $e = d$ in Eq. (1.1), then it reduces to a generalized (3 + 1)-dimensional KP equation, which can be found in reference [57]. If we put $z = y, d = 1, e = 1$ to the (3 + 1)-dimensional KS equation, Eq. (1.1) converted to the (2 + 1)-dimensional KS equation involving the second-order dispersion term (u_{yy}). But if we set $z = x$ keeping fixed other values to the (3 + 1)-dimensional original KS equation, Eq. (1.1) also converted to the (2 + 1)-dimensional KS equation involving two second-order dispersion terms u_{xx} and u_{yy}, which is different from the existing literature. Based on refs. [35,39,58], we consider a dimensionally reduced (2 + 1)-dimensional KS equation for $z = x$ for this study to examine the localized wave and their interaction solutions. The equation becomes

$$(u_t + \alpha u u_x + \gamma u_{xxx})_x + d u_{yy} + e u_{xx} = 0. \tag{1.2}$$

In the past, several authors [35,39,58] converted dimensionally reduced form of the NLEEs. Lie et al., [58] obtained the localized waves and interaction solutions with the help of HBM from the reduced form of (3 + 1)-dimensional generalized Kadomtsev-Petviashvili (gKP) equation after setting $z = x$. Kumar et al., [39] reduced the (3 + 1)-dimensional Boussinesq equation (BqE) dimensionally after substituting $z = y$, and Wu et al., [35] reduced the (3 + 1)-dimensional Boiti-Leon-Mana-Pempinelli (BLMP) equation dimensionally after setting $z = x$ and $z = 0$ to construct the localized and their interaction solutions to the BqE and BLMP equations.

To the author's best knowledge, the dimensionally reduced (2 + 1)-dimensional KS equation has never been studied for generating localized waves and their interaction solutions. In this paper, we will discuss the localized waves and their variety of interaction solutions from *N*-soliton using the help of the long-wave limit approach to dimensionally reduced (2 + 1)-dimensional KS equation. The exhibited outcomes reveal that the attained solitons might help explain the propagation of nonlinear waves in a bubbly liquid.

The outline of this paper is organized as follows: In section 2, we first present the *N*-soliton solutions of (3 + 1)-dimensional KS equation and its dimensionally reduced form via the HBM. Section 3 deals with localized waves and their variety of interactions among *N*-soliton solutions to the reduced dimensionally KS equation using the long-wave limit approach and some restriction parameters. Finally, the discussion of the outcomes and the conclusion are found in section 4.

Dimensionally reduced form of (2 + 1)-D KS equation and its *N*-soliton solutions

By applying the dependent variable transformation [43]:

$$u = \frac{12\gamma}{\alpha}(\ln f)_{xx}, \tag{2.1}$$

where $f(x, y, z)$ is the unfamiliar function of x, y, z, and time t. If we put Eq. (2.1) into Eq. (1.1), then the HBM is given as:

$$\left(D_x D_t + \gamma D_x^4 + d D_y^2 + e D_z^2\right)(f.f) = 0, \tag{2.2}$$

where $D_s(s = x, y, z, t)$ is the Hirota bilinear operator, which can be written as

$$D_x^{\alpha} D_y^{\beta} D_z^{\gamma} D_t^{\eta}(f.g) = (\partial_x - \partial_{x'})^{\alpha}\left(\partial_y - \partial_{y'}\right)^{\beta}(\partial_z - \partial_{z'})^{\gamma}(\partial_t - \partial_{t'})^{\eta} f(x, y, z, t)\, g(x', y', z', t')|_{x=x', y=y', z=z', t=t'}, \tag{2.3}$$

where α, β, γ, and η are all non-negative integers.

Based on HBM, *N*-order soliton solutions of Eq. (1.2) can be determined in Eq. (2.2) and Eq. (2.3), where f can be written as

$$f_i = 1 + \sum_{i=1}^{N} e^{v_i} + \sum_{i<j}^{N} A_{ij} e^{(v_i + v_j)} + \sum_{i<j<k}^{N} A_{ij}A_{ik}A_{jk} e^{(v_i + v_j + v_k)} + \cdots + \left(\prod_{i<j} A_{ij}\right)\left(e^{\sum_{i=1}^{N} v_i}\right), \tag{2.4}$$

and the dispersion variables (v_i) and generalized phase shifts (A_{ij}) can be expressed as

$$v_i = p_i x + q_i y + h_i z + \eta_i t + \omega_i, i = 1,2,3,4,\cdots\cdots.., N,$$

$$A_{ij} = \frac{3\gamma\left(p_i^2 p_j - p_i p_j^2\right)^2 - d\left(p_i q_j - p_j q_i\right)^2 - e\left(h_i p_j - h_j p_i\right)^2}{3\gamma\left(p_i^2 p_j + p_i p_j^2\right)^2 - d\left(p_i q_j - p_j q_i\right)^2 - e\left(h_i p_j - h_j p_i\right)^2}, i,j = 1,2,\cdots.,N. \tag{2.5}$$

$$\eta_i = \frac{1}{p_i}\left(\gamma p_i^4 + d q_i^2 + e h_i^2\right),$$

where the constants p_i, q_i, h_i, and ω_i are parameters related to the phase and amplitude of the i th soliton.

Without losing generality, if we put $z = x$ in Eq. (2.2) then it can be transformed into the following HBE:

$$\left(D_x D_t + \gamma D_x^4 + d D_y^2 + e D_x^2\right)(f.f) = 0. \tag{2.6}$$

Also, the generalized phase shifts and dispersion variables are changeable because of the given solution of Eq. (2.6), then it becomes:

$$f_N = 1 + \sum_{i=1}^{N} e^{v_i} + \sum_{i<j}^{N} A_{ij} e^{\left(v_i + v_j\right)} + \sum_{i<j<k}^{N} A_{ij}A_{ik}A_{jk} e^{\left(v_i+v_j+v_k\right)} + \cdots + \left(\prod_{i<j} A_{ij}\right)$$

$$\left(e^{\sum_{i=1}^{N} v_i}\right), \tag{2.7}$$

$$\text{where} v_i = p_i x + q_i y - \frac{1}{p_i}\left(\gamma p_i^4 + d q_i^2 + e p_i^2\right)t + \omega_i, \text{ i} = 1, 2, 3, 4, \cdots\cdots.., \text{N}. \tag{2.8}$$

$$A_{ij} = \frac{3\gamma\left(p_i^2 p_j - p_i p_j^2\right)^2 - d\left(p_i q_j - p_j q_i\right)^2}{3\gamma\left(p_i^2 p_j + p_i p_j^2\right)^2 - d\left(p_i q_j - p_j q_i\right)^2}, i,j = 1,2,3,4,\cdots\cdots,N. \tag{2.9}$$

By using Eq. (2.7) into (2.9) in Eq. (2.1), we can determine the following N-soliton solutions of Eq. (1.2)

$$u = \frac{12\gamma}{\alpha}\left(\ln f_N\right)_{xx}, i = 1,2,3,\cdots\cdots\cdots.,N. \tag{2.10}$$

If we put $N = 1$, $N = 2$, $N = 3$, and $N = 4$, the solution of u is given by Eq. (1.2) which represents one, two, three, and four soliton solutions and those solutions are displayed in Fig. 1**(a)-(h)** under suitable parameters $p_1 = 1$, $p_2 = -2$, $p_3 = 3$, $p_4 = 4$, $q_1 = 1, q_2 = 2, q_3 = -3$, $q_4 = 3, \omega_1 = 0, \omega_2 = 0, \omega_3 = 0, \omega_4 = 0, \alpha = 1, \gamma = 1, b = 1, d = 1$, and $e = 1$. Moreover, Fig. 1**(e)-(h)** exhibit the density plot that corresponds to Fig. 1**(a)-(d).** However, from Fig. 1**(a)-(h)** that the velocity and amplitude are the same but propagation is different when $t < 0$ and $t > 0$.

Interaction solutions and localized waves from N-soliton solutions

In this part, we investigate the interaction solutions and localized waves from N-soliton solutions among two, three, and four-line solitons.

Localized waves between two solitons

In this part, we obtained two cross-line solitons, two-parallel line solitons, x-periodic breather (PB) soliton, y-PB soliton,xy-PB soliton, and one lump soliton solution of Eq. (1.2). If we set $N = 2$ in Eq. (2.7), the function f_2 can be written as

$$f_2 = 1 + e^{v_1} + e^{v_2} + A_{12} e^{v_1 + v_2}. \tag{3.1}$$

Now, setting Eq. (3.1) into Eq. (2.1) then the solution of two solitons can be expressed as follows:

$$u = \frac{12\gamma}{\alpha}\left(\ln f_2\right)_{xx}. \tag{3.2}$$

Family-I: Interaction solutions of two cross-line and two parallel-line solitons (LS)

To determine the interaction of two cross-LS and parallel-LS for Eq. (2.1), the parameters p_i, q_i, and ω_i must meet the following requirements

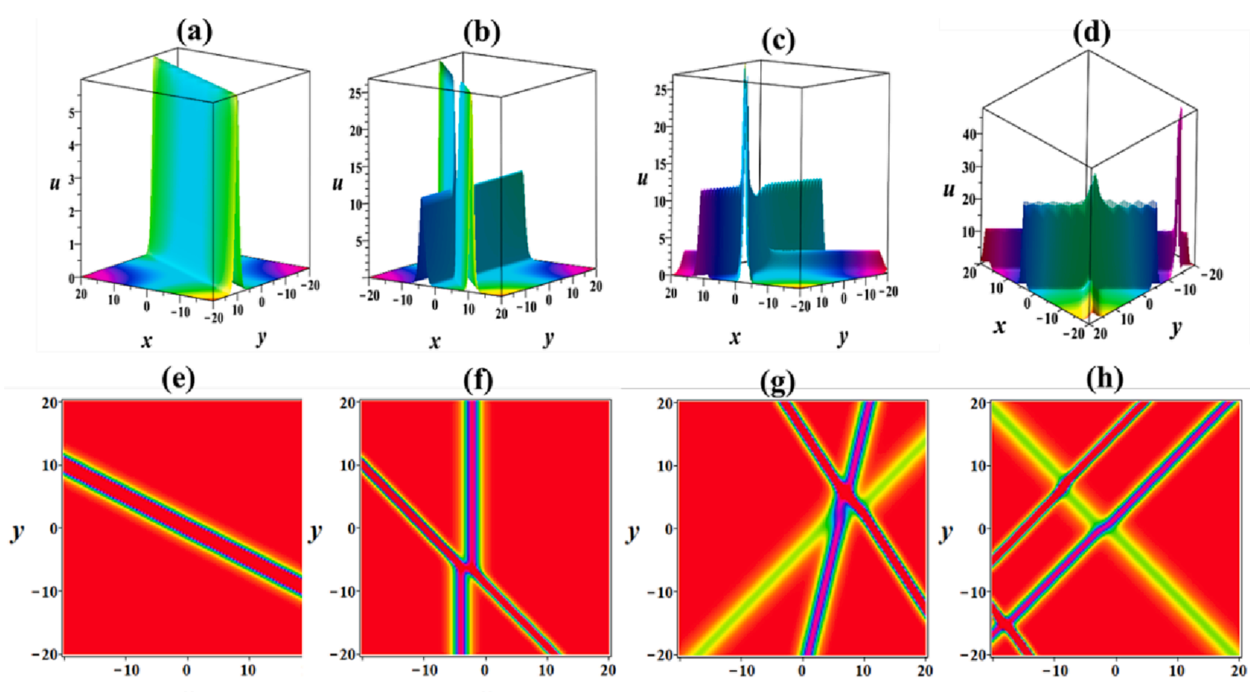

Fig. 1. Graphical representations of N-soliton solutions via the Eq. (2.10) of Eq. (1.2) in the (x, y) plane when $t = 2$ with $p_1 = 1$, $p_2 = -2$, $p_3 = 3$, $p_4 = 4$, $q_1 = 1, q_2 = 2, q_3 = -3, q_4 = 3, \omega_1 = 0, \omega_2 = 0, \omega_3 = 0, \omega_4 = 0, \alpha = 1, \gamma = 1, b = 1, d = 1$, and $e = 1$: 3D plot for (a) $N = 1$, (b) $N = 2$, (c) $N = 3$, and (d) $N = 4$. (e)-(h) the corresponding density plot of (a)-(d).

$p_i = r_i, q_i = s_i, (i = 1, 2),$

where two real constants are r_i and s_i; $r_i \neq 0$ and $s_1 \neq s_2$.

(i) For two cross-LS: The cross-LS is maintained the following structure

$(r_1 s_2 - r_2 s_1) \neq 0$. If we put $r_1 = 3, r_2 = -2, s_1 = 3, s_2 = 0$, $\omega_1 = 0$, $\omega_2 = 0, \alpha = 1, \gamma = 1, b = 1, d = 1$, and $e = 1$ in Eq. (3.2), then Eq. (3.2) becomes

$$u = 12\left(\ln\left(1 + e^{3x+3y-33t} + e^{-2x+10t} + 37e^{x+3y-23t}\right)\right)_{xx}. \tag{3.3}$$

3D and density plots for the interaction of two cross-LS solutions are presented by Eq. (3.3) in Fig. 2 **(a)-(f)** for varying time $t = -1, t = 0, t = 1$. Fig. 2**(d)-(f)** show the density plots of the two cross-LS presented in Fig. 2**(a)-(c)**. In addition, two LS are crossly meet with each other (see Fig. 2**(a)-(f)**). It is also seen that one LS propagates along the x-axis with a negative direction and is perpendicular to it, while the other soliton propagates along the x-axis with a positive direction.

(ii) For two parallel soliton molecules

The parallel two soliton molecules satisfy the following conditions $(r_1 - r_2)(s_1 - s_2) \neq 0$, but $r_1 s_2 - r_2 s_1 = 0$. As per aforesaid rules, if we set $r_1 = 5, r_2 = -3, s_1 = -5, s_2 = 3$, $\omega_1 = 0, \omega_2 = 0, \alpha = 1, \gamma = 1, b = 1, d = 1$, and $e = 1$ in Eq. (3.2), then Eq. (3.2) becomes

$$u = 12\left(\ln\left(1 + e^{5x-5y-135t} + e^{-3x+3y+33t} + 16e^{2x-2y-102t}\right)\right)_{xx}. \tag{3.4}$$

Fig. 3**(a)-(f)** exhibit the interactions of two parallel soliton molecules, which are depicted as a density plot and 3D plot in the (x, y) plane. Besides, Fig. 3**(d)-(f)** illustrates the density plot that corresponds to Fig. 3**(a)-(c).** At time $t < 0$, two parallel soliton molecules are divided with one highest amplitude and another with the lowest amplitude. It can be seen that at $t = 0$, these LSs are overlapping with each other. It is also seen that at $t > 0$, two soliton molecules are separated from each other but the soliton position change at time $t < 0$. Moreover, the shape and amplitude keep unchanged when it propagates for $t < 0$ and $t > 0$ but the position of solitons is changed. The figures are not attached here because due to space consumption.

Family-II: One y-periodic breather (PB) solution

To investigate one y-PB wave solution for Eq. (1.2), this maintained the following structure for Eq. (3.2) into Eq. (3.1):

$$p_1 = p_2 = l_1, q_1 = q_2^* = Is_1, \omega_1 = \omega_2 = 0, \text{and} l_1 \neq 0, s_1 \neq 0,$$

where '*' denotes the conjugate of a complex number and $I^2 = -1$.

Substituting the values of parameters $l_1 = 3, s_1 = \frac{1}{2}, \omega_1 = 0, \omega_2 = 0$, $\alpha = 1, \gamma = 1, b = 1, d = 1$, and $e = 1$ in Eq. (3.2), then it becomes in the following form

$$u = 12\left(\ln\left(1 + \frac{48}{49}e^{\frac{139}{4}t+x} + e^{\frac{139}{8}t+\frac{1}{2}x+3Iy} + e^{\frac{139}{8}t+\frac{1}{2}x-3Iy}\right)\right)_{xx}. \tag{3.5}$$

Fig. 4**(a)-(f)** represent one y-PB wave solution, which is shown by Eq. (3.5) and displayed by density and 3D plots. For better understanding, Fig. 4**(d)-(f)** illustrate the density views from Fig. 4**(a)-(c)**. The given one y-PB wave solution moves always perpendicular to the y-axis with varying times $t = -1$, $t = 0$, and $t = 1$, respectively (see Fig. 4**(a)-(f)**). The position of the y-PB wave is shifted from the positive to the negative direction at various times $(t = -1, 0, 1)$. Moreover, both the amplitude and shape of the y-PB wave remain constant.

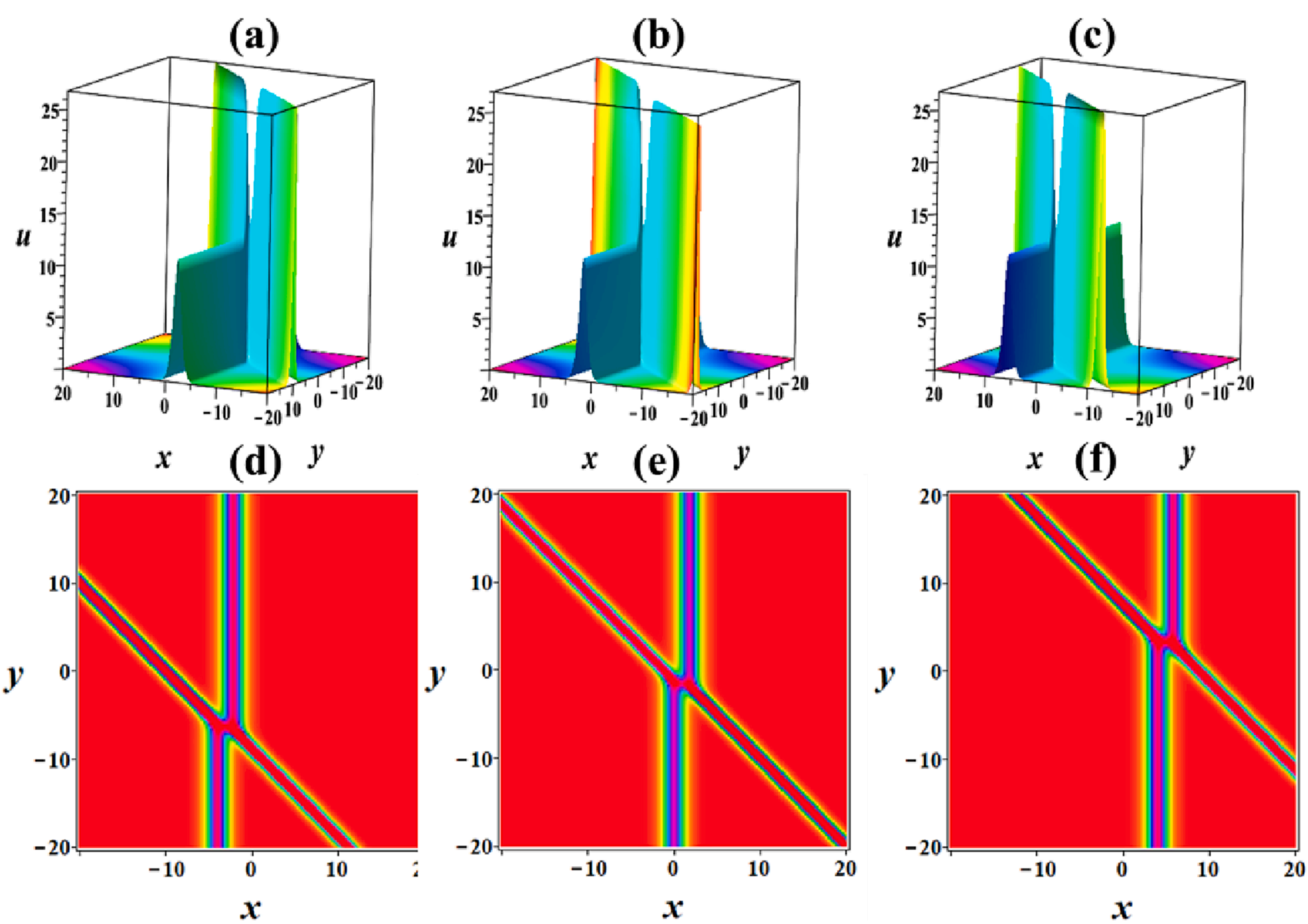

Fig. 2. The profile of two cross-line soliton solutions via Eq. (3.3) in the (x, y) plane with $r_1 = 3$, $r_2 = -2, s_1 = 3, s_2 = 0$, $\omega_1 = 0, \omega_2 = 0, \alpha = 1, \gamma = 1, b = 1, d = 1$, and $e = 1$: 3D plot for (a) $t = -1$, (b) $t = 0$, and (c) $t = 1$. (d)-(f) the corresponding density plot of (a)-(c).

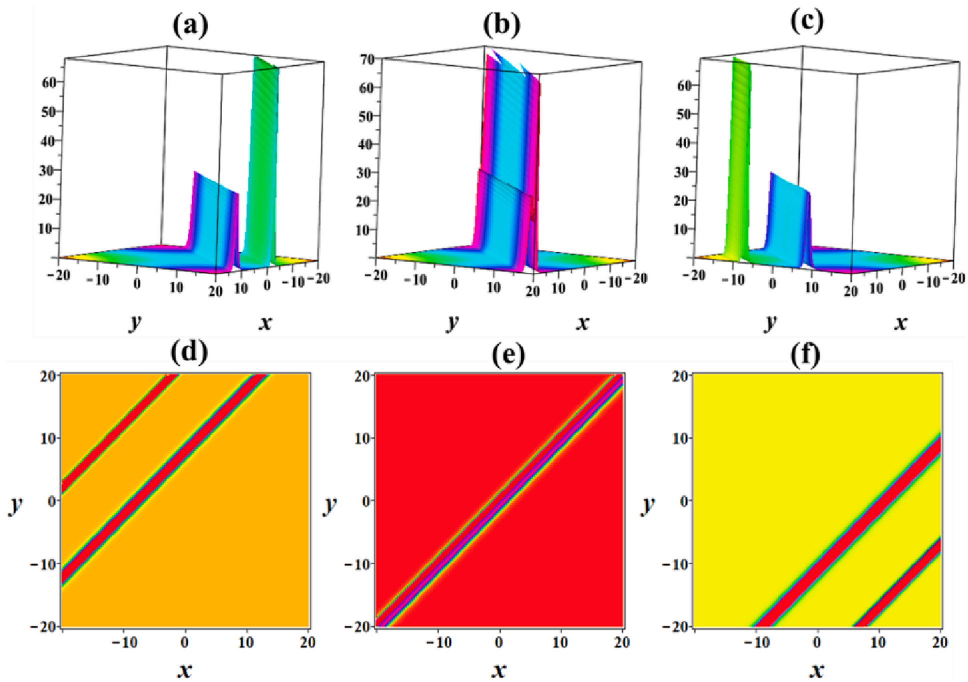

Fig. 3. The profile of two parallel soliton molecules solution via Eq. (3.4) in the $(\mathbf{x}, \mathbf{y})$ plane with $r_1 = 5, r_2 = -3, s_1 = -5, s_2 = 3, \omega_1 = 0, \omega_2 = 0, \alpha = 1, \gamma = 1, b = 1, d = 1$, and $e = 1$: 3D plot for (a) $t = -1$, (b) $t = 0$, and (c) $t = 1$. (d)-(f) the corresponding density plot of (a)-(c).

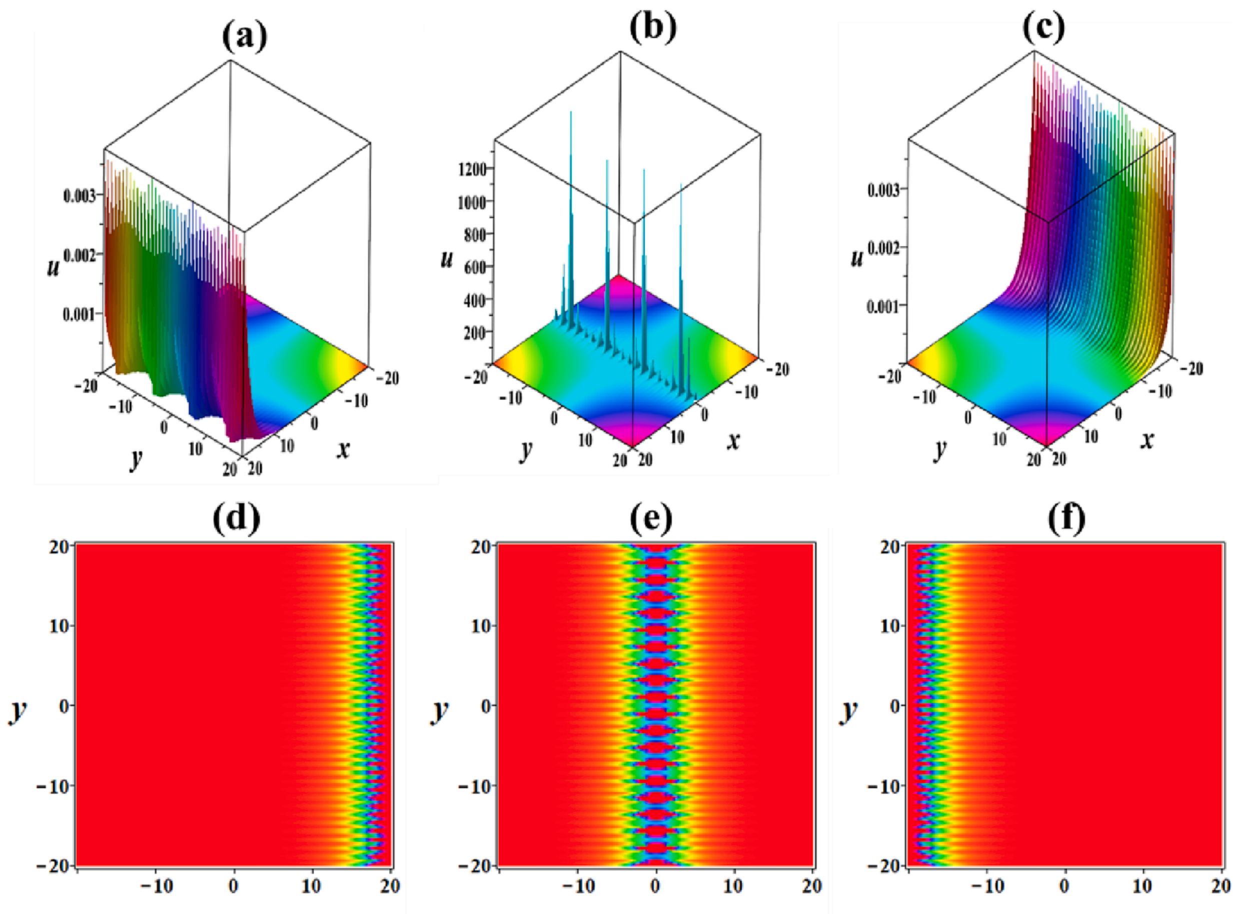

Fig. 4. The profile of one $\mathbf{y}$-periodic breather solution $|u(x, y, t)|$ via Eq. (3.5) in the $(\mathbf{x}, \mathbf{y})$ plane with $l_1 = 3, s_1 = \frac{1}{2}, \omega_1 = 0, \omega_2 = 0, \alpha = 1, \gamma = 1, b = 1, d = 1$, and $e = 1$: 3D plot for (a) $t = -1$, (b) $t = 0$, and (c) $t = 1$. (d)-(f) the corresponding density plot of (a)-(c).

Family-III: Interaction solutions between one $(\mathbf{x},\mathbf{y})$-PB wave and one x-PB wave

To obtain one (x,y)-PB wave solution of Eq. (1.2), satisfies the following structure for Eq. (3.2) into Eq. (3.1):

$$p_1 = p_2 = l_1,\ q_1 = q_2^* = r_1 + Is_1,\ \omega_1 = \omega_2 = 0,\ \text{and}\ l_1 \neq 0, r_1 \neq 0, s_1 \neq 0, \tag{3.6}$$

If we put $l_1 = \frac{1}{6}, r_1 = \frac{1}{3}, s_1 = 1, \omega_1 = 0, \omega_2 = 0, \alpha = 1, \gamma = 1, b = 1, d = 1$, and $e = 1$ in Eq. (3.2), then it becomes in the following form:

$$u = 12\left(\ln\left(1 + \frac{432}{433}e^{\frac{1115}{108}t+\frac{1}{3}x+\frac{2}{3}y} + e^{\left(\frac{1115}{216}+4I\right)t+\frac{1}{6}x+\left(\frac{1}{3}-I\right)y} + e^{\left(\frac{1115}{216}-4I\right)t+\frac{1}{6}x+\left(\frac{1}{3}+1\right)y}\right)\right)_{xx}. \tag{3.7}$$

Fig. 5**(a) and 5(c)** represent one (x,y)-PB wave solution, which is specified by Eq. (3.7) and displayed by 3D and density plots. On the other side, we have investigated the x-PB wave for Eq. (1.2), which maintained the following structure for Eq. (3.2) into Eq. (3.1):

$$p_1 = p_2^* = Im_1, q_1 = s_1, q_2 = s_1, \omega_1 = \omega_2 = 0,\ \text{and}\ m_1 \neq 0, s_1 \neq 0 \tag{3.8}$$

Substituting the value of $m_1 = \frac{1}{2}, s_1 = 3, \omega_1 = 0, \omega_2 = 0, \alpha = 1, \gamma = 1, b = 1, d = 1$, and $e = 1$ in Eq. (3.2), it turns in the following form:

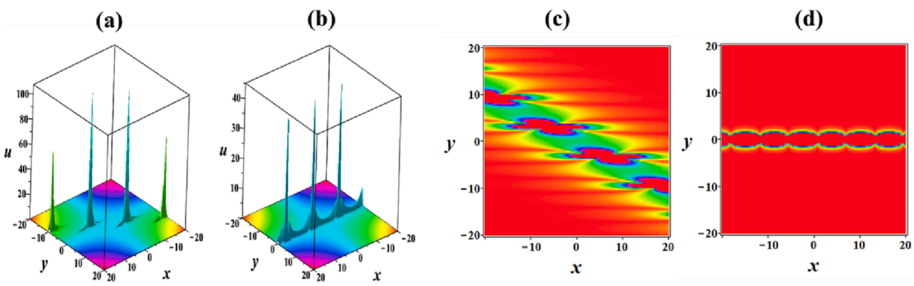

Fig. 5. Profile of periodic breather solution $|u(x,y,t)|$ at $t = 0$. 3D plot of (a) one $(\mathbf{x},\mathbf{y})$-periodic breather solution via Eq. (3.7) with $l_1 = \frac{1}{6}, r_1 = \frac{1}{3}, s_1 = 1, \omega_1 = 0, \omega_2 = 0, \alpha = 1, \gamma = 1, b = 1, d = 1, e = 1$, and (b) one **x**-periodic breather solution via the Eq. (3.10) with $m_1 = \frac{1}{2}, s_1 = 3, \omega_1 = 0, \omega_2 = 0, \alpha = 1, \gamma = 1, b = 1, d = 1, e = 1$.(c)-(d) corresponding density plot of (a)-(b).

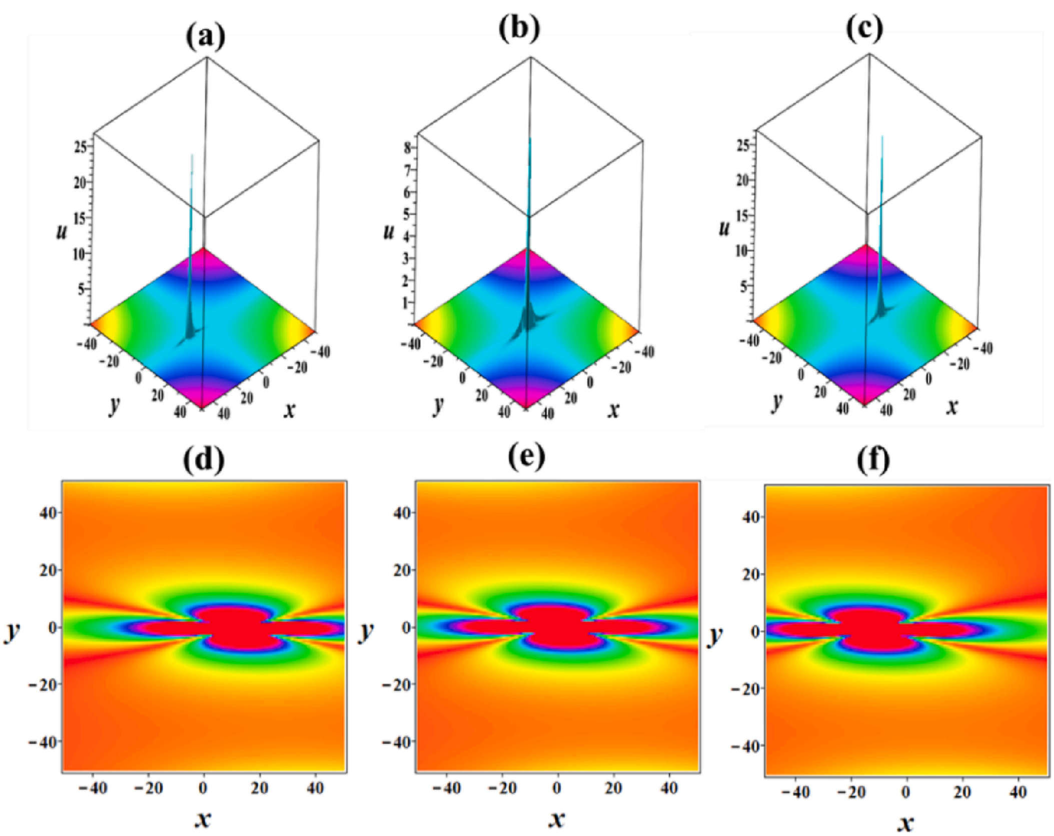

Fig. 6. The profile of lump soliton solution $|u(x,y,t)|$ via Eq. (3.11) in the $(\mathbf{x},\mathbf{y})$ plane with $l_1 = \frac{1}{5}, l_2 = 2, r_1 = \frac{1}{2}, s_1 = 5, \omega_1 = \omega_2^* = I\pi, \alpha = 1, \gamma = 1, b = 1, d = 1$, and $e = 1$: 3D plot for (a) $t = -0.5$, (b) $t = 0$, and (c) $t = 0.5$. (d)-(f) the corresponding density plot of (a)-(c).

$$u = 12\left(\ln\left(1 + e^{\frac{141}{8}It + \frac{1}{2}Ix + 3y} + e^{-\frac{141}{8}It - \frac{1}{2}Ix + 3y} + \frac{47}{48}e^{6y}\right)\right)_{xx}. \tag{3.9}$$

Fig. 5**(b) and 5(d)** represent one x-PB wave solution, which is specified by Eq. (3.9) and displayed by 3D and density plots. Moreover, the amplitude and the shape of the x-PB wave is the same but their position changes at various time.

Family-IV: Lump soliton and rogue wave solutions

To obtain one lump soliton for Eq. (1.2), if setting parameters $q_1 = m_1p_1, q_2 = m_2p_2,\ p_1 = l_1\varepsilon, p_2 = l_2\varepsilon$, and $\omega_1 = \omega_2^* = \pi i$ in Eq. (2.7), then the function f_2 can be written as

$$f_2 = (V_1V_2 + a_{12})l_1l_2\varepsilon^2 + O(\varepsilon^3). \tag{3.10}$$

Taking the limit as $\varepsilon \to 0$ in Eq. (3.10), then the lump soliton solution of Eq. (1.2) can be determined in the following from Eq. (3.2):

$$u = \frac{12\gamma}{\alpha}(\ln(V_1V_2 + a_{12}))_{xx}, \tag{3.11}$$

where,

$$V_i = x + m_iy - \left(e + m_i{}^2d + \gamma\right)t, i = 1, 2, \tag{3.12}$$

$$a_{12} = \frac{1}{d(m_1 - m_2)^2}. \tag{3.13}$$

Substituting the parameters $m_1 = m_2^* = r_1 + Is_1; (s_1 \neq 0)$ to (3.13)-(3.10), we find that a one-lump soliton will result from the collapse of the two-soliton solution. Taking $l_1 = \frac{1}{5}, l_2 = 2, r_1 = \frac{1}{2}, s_1 = 5, \omega_1 = \omega_2^* = I\pi, \alpha = 1, \gamma = 1, b = 1, d = 1$, and $e = 1$ to the Eqs. (3.13)-(3.10), we can find a lump soliton solution. Fig. 6**(a)-(f)** represent a lump soliton solution, which is specified by Eq. (3.11) and displayed by 3D and density plots. In addition, Fig. 6**(d)-(f)** display the density plot that corresponds to Fig. 6**(a)-(c)**. Besides, the lump wave maintained one crest and two trough positions (see Fig. 6**(a)-(f)**). It is also seen from Fig. 6 that the lump wave preserves its original size and shape, but the position is changed at various times at $t = -5$, $t = 0$, and $t = 5$.

On the other hand, we can investigate the rogue wave solution from Eq. (1.2) through the class of solution u given by Eq. (3.11), if we choose the value of m_1 and m_2 are all only real constants. According to the rule of mention, we can be obtained a rogue wave solution, which is shown in Fig. 7**(a)-(f)**, If we put $s_1 = 0$ and other parameters $l_1 = \frac{1}{5}, l_2 = 2, r_1 = \frac{1}{2}$, $\omega_1 = \omega_2^* = I\pi, \alpha = 1, \gamma = 1, b = 1, d = 1$, and $e = 1$ in Eq. (3.11). From Fig. 7 **(a)-(f),** we can be seen that the amplitude and shape of rogue waves are changed but their position are unchanged with different times at $t = -1, t = 0$, and $t = 1$. Table 1 provides some mathematical aspects for the selecting proper parameters to produce localized wave and interaction solutions with the two soliton solutions of Eq. (1.2).

Localized waves between three solitons

In this subsection, we obtain localized waves and their interaction solutions among three solitons as well as their explanation of graphs shown by the KSE. The specific localized waves and their interaction solutions, viz. three cross-LS, the intersection between two parallel and one-LS, three parallel-LS, the interaction between one LS and one PB, one lump and one-LS. If we set $N = 3$ in Eq. (2.7), then the function f_3 can be written as:

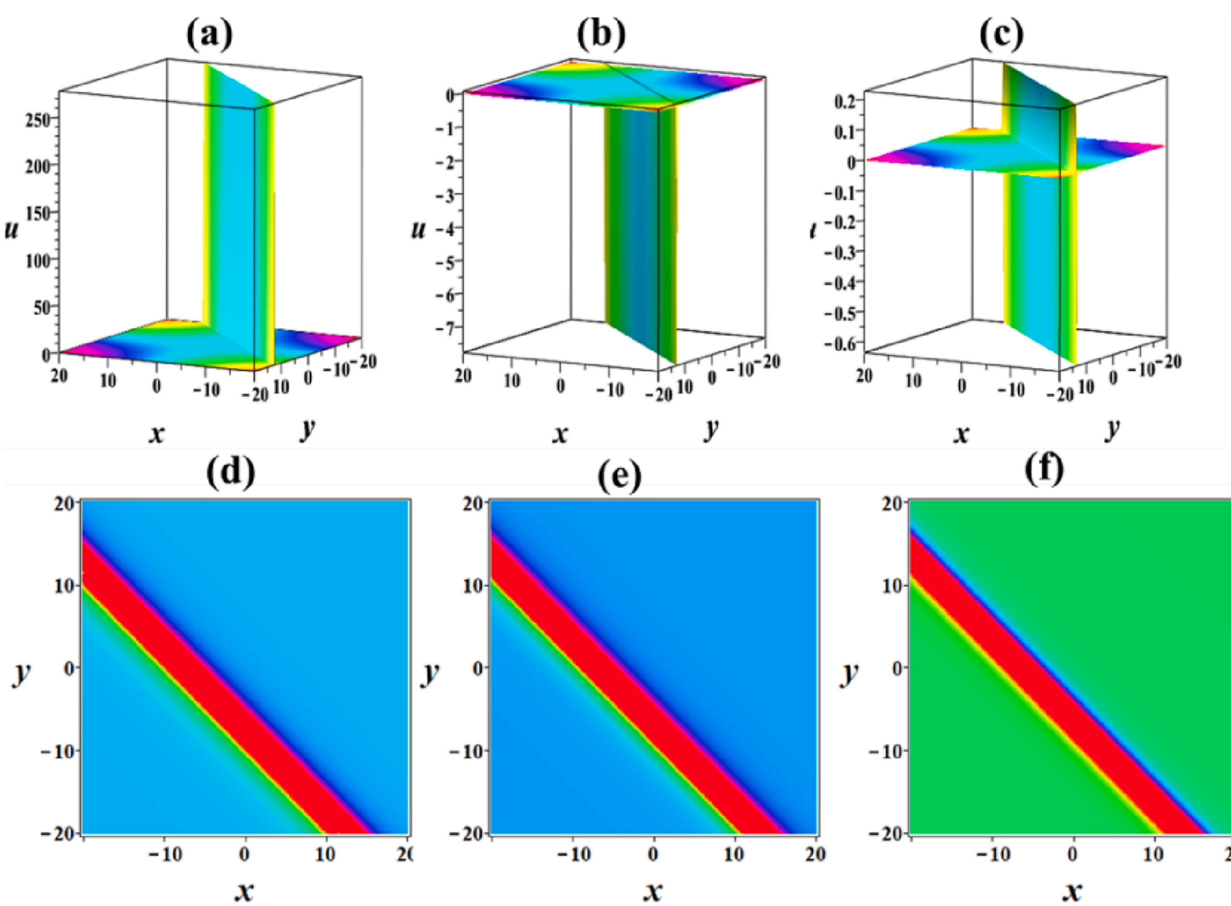

Fig. 7. The profile of line rogue wave solution $|u(x,y,t)|$ via Eq. (3.11) in the (x,y) plane with $l_1 = \frac{1}{5}, l_2 = 2, r_1 = \frac{1}{2}, s_1 = 0, \omega_1 = \omega_2^* = I\pi, \alpha = 1, \gamma = 1, b = 1, d = 1$, and $e = 1$: 3D plot for (a) $t = -1$, (b) $t = 0$, and (c) $t = 1$. (d)-(f) the corresponding density plot of (a)-(c).

Table 1
Various localized wave forms and their interaction solutions between two solitons.

N-soliton	Localized wave forms	Parameters
$N = 2$	Two LS	$p_1 = r_1, p_2 = r_2, q_1 = s_1, q_2 = s_2, \omega_1 = \omega_2 = 0$.Cross-LS: $(r_1 s_2 - r_2 s_1) \neq 0$. Parallel-LS: $(r_1 - r_2)(s_1 - s_2) \neq 0$; but $r_1 s_2 - r_2 s_1 = 0$.
	One *y*-PB	$p_1 = p_2 = l_1,\ q_1 = q_2^* = Is_1,\ \omega_1 = \omega_2 = 0$, and $l_1 \neq 0, s_1 \neq 0$.
	One *x*-PB	$p_1 = p_2^* = Im_1,\ q_1 = s_1,\ q_2 = s_1,\ \omega_1 = \omega_2 = 0$, and $m_1 \neq 0,\ s_1 \neq 0$.
	One (x, y)-PB	$p_1 = p_2 = l_1, q_1 = q_2^* = r_1 + Is_1,\ \omega_1 = \omega_2 = 0$, and $l_1 \neq 0, r_1 \neq 0, s_1 \neq 0$.
	One lump soliton	$q_i = m_i p_i, p_i = l_i \varepsilon\ (i = 1,\ 2), m_1 = m_2^* = r_1 + Is_1, \omega_1 = \omega_2^* = I\pi$, and $\varepsilon \to 0$.

$$f_3 = 1 + e^{v_1} + e^{v_2} + e^{v_3} + A_{12} e^{v_1 + v_2} + A_{13} e^{v_1 + v_3} + A_{23} e^{v_2 + v_3} + A_{123} e^{v_1 + v_2 + v_3}, \tag{3.14}$$

where v_i and A_{ij} are shown in Eq. (2.8) and Eq. (2.9) and the phase shift contains $A_{123} = A_{12} A_{23} A_{13}$. Now, putting Eq. (3.14) into Eq. (2.10), then three soliton solutions of Eq. (1.2) can be expressed as:

$$u = \frac{12\gamma}{\alpha} (\ln f_3)_{xx} \tag{3.15}$$

Family-I: Interaction between three-LS solutions

To investigate the interaction between three-LS solutions for Eq. (1.2), the parameters p_i, q_i, and ω_i must meet the following requirements for Eq. (3.15):

$$p_i = r_i, q_i = s_i, (i = 1, 2, 3), \text{ and } \omega_1 = \omega_2 = \omega_3 = 0, \tag{3.16}$$

where two real constants are r_i and s_i.

(i) For three cross-LS solutions

The three cross-LS solutions are maintained the following structure as $\prod_{i \neq j} (r_i s_j - r_j s_i) \neq 0$. If we put $r_1 = 3, r_2 = 1, r_3 = 2, s_1 = 2, s_2 = -1$, $s_3 = -\frac{1}{2}, \omega_1 = 0, \omega_2 = 0, \omega_3 = 0, \alpha = 1, \gamma = 1, b = 1, d = 1$, and $e = 1$ in Eq. (3.16), then we can determine the three cross-LS solutions which as follows:

$$u = 12\left(\ln\left(1 + e^{-\frac{94}{3}t + 3x + 2y} + e^{-3t + x - y} + e^{-\frac{81}{8}t + 2x - \frac{1}{2}y} + \frac{83}{407} e^{-\frac{103}{3}t + 4x + y} + \frac{83}{407} e^{-\frac{995}{24}t + 5x + \frac{3}{2}y} + \frac{83}{407} e^{-\frac{105}{8}t + 3x - \frac{3}{2}y} + \frac{571787}{67419143} e^{-\frac{1067}{24}t + 6x + \frac{1}{2}y}\right)\right)_{xx}. \tag{3.17}$$

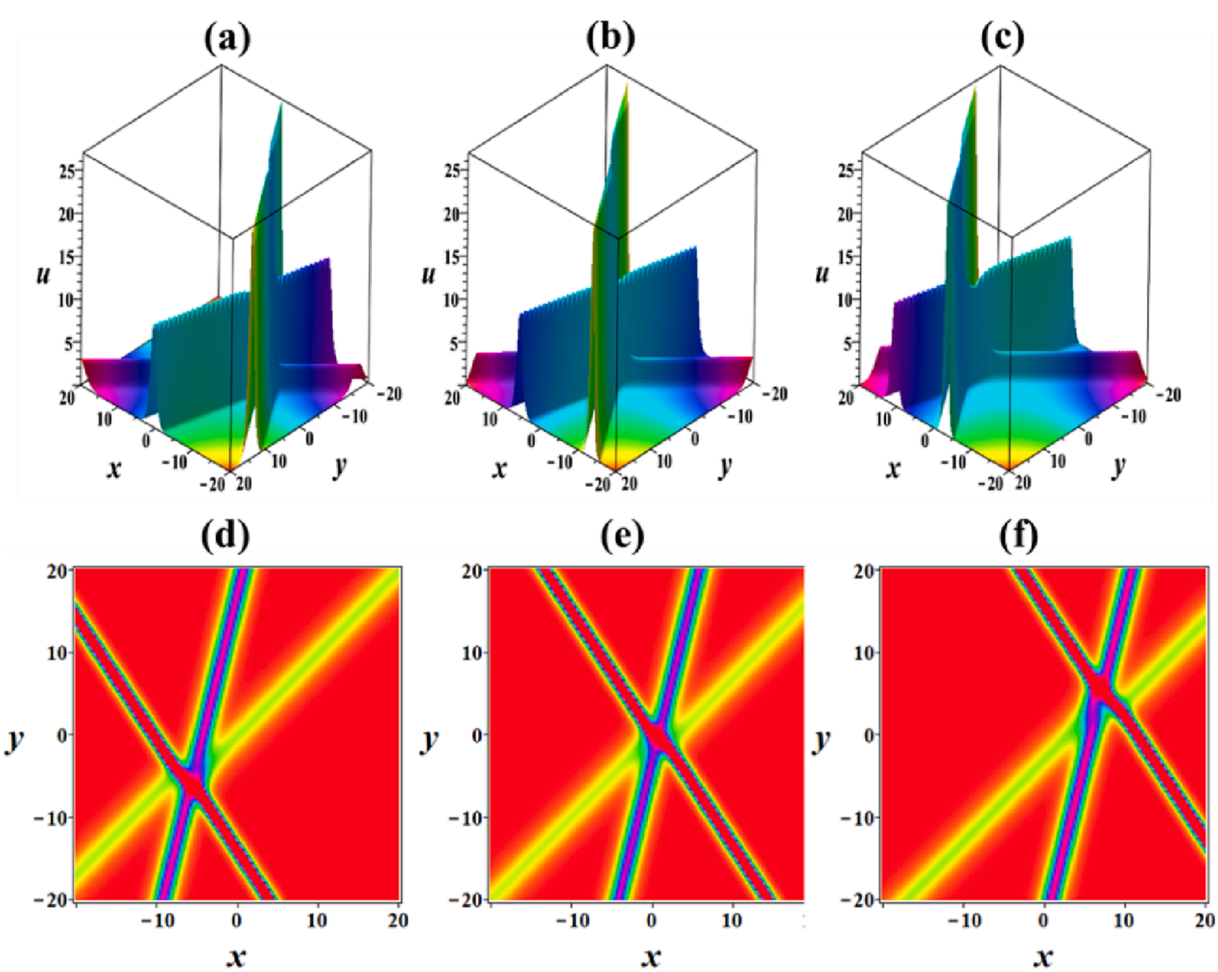

Fig. 8. The profile of three cross-line soliton solutions via Eq. (3.17) in the $(\mathbf{x}, \mathbf{y})$ plane with $r_1 = 3$, $r_2 = 1, r_3 = 2, s_1 = 2, s_2 = -1, s_3 = -\frac{1}{2}, \omega_1 = 0, \omega_2 = 0, \omega_3 = 0, \alpha = 1, \gamma = 1, b = 1, d = 1$, and $e = 1$: 3D plot for (a) $t = -1$, (b) $t = 0$, and (c) $t = 1$. (d)-(f) the corresponding density plot of (a)-(c).

Fig. 8**(a)-(f)** represent three cross-LS solutions, which are indicated by Eq. (3.17) and shown by 3D and density plots. In addition, Fig. 8**(d)-(f)** displays the density plot that corresponds to Fig. 8**(a)-(c)**. It can be seen from the above graphs that the shape and amplitude of three LS keep unchanged but their position changed with varying time $t = -1, t = 0, t = 1$, respectively.

(ii) For interaction between two parallel-LS and one-LS solutions

In this part, we obtain the interaction between two parallel-LS and one-LS, which is presented by the structure $\prod_{i\neq j}(r_i s_j - r_j s_i) = 0$ and $\sum_{i\neq j}(r_i s_j - r_j s_i)^2 \neq 0$. Taking $r_1 = 3, r_2 = 2, r_3 = -1, s_1 = 3, s_2 = 2, s_3 = 1, \omega_1 = 0, \omega_2 = 0, \omega_3 = 0, \alpha = 1, \gamma = 1, b = 1, d = 1,$ and $e = 1$ in Eq. (3.15), then we can find an intersection between two parallel and one LS solution becomes:

Here, the obtained solution of Eq. (3.18) is shown by the 3D and density plots, which is presented in Fig. 9**(a)-(f)** with various time at $t = -1, t = 0, t = 1$. In addition, Fig. 9**(d)-(f)** display the density plot that corresponds to Fig. 9**(a)-(c)**. At $t = 0$, we can see the intersection between overlapping two LS and one LS as shown in Fig. 9**(e)**. Moreover, with varying time ($t = -1$ and $t = 1$), the amplitude and shape of interaction between two parallel and one LS keep unchanged but their position is changed.

(iii) For three parallel soliton molecules solution

To obtain the three parallel soliton molecules, which maintained the following structure $\sum_{i\neq j}(r_i s_j - r_j s_i)^2 = 0$. If taking $r_1 = 3, r_2 = 1, r_3 = 2, s_1 = 3, s_2 = 1, s_3 = 2, \omega_1 = 0, \omega_2 = 0, \omega_3 = 0, \alpha = 1, \gamma = 1, b = 1, d = 1,$ and $e = 1$ in Eq. (3.16), then the three parallel soliton molecules solution is

$$u = 12\left(\ln\left(1 + e^{-33t+3x+3y} + e^{-3t+x+y} + e^{-12t+2x+2y} + \frac{1}{4}e^{-36t+4x+4y} + \frac{1}{4}e^{-45t+5x+5y} + \frac{1}{4}e^{-15t+3x+3y} + \frac{1}{64}e^{-48t+6x+6y}\right)\right)_{xx}. \tag{3.19}$$

$$u = 12\left(\ln\left(1 + e^{-33t+3x+3y} + e^{-12t+2x+2y} + e^{3t-x+y} + \frac{1}{25}e^{-45t+5x+5y} + \frac{1}{25}e^{-30t+2x+4y} + \frac{1}{25}e^{-9t+x+3y} + \frac{1}{15625}e^{-42t+4x+6y}\right)\right)_{xx}. \tag{3.18}$$

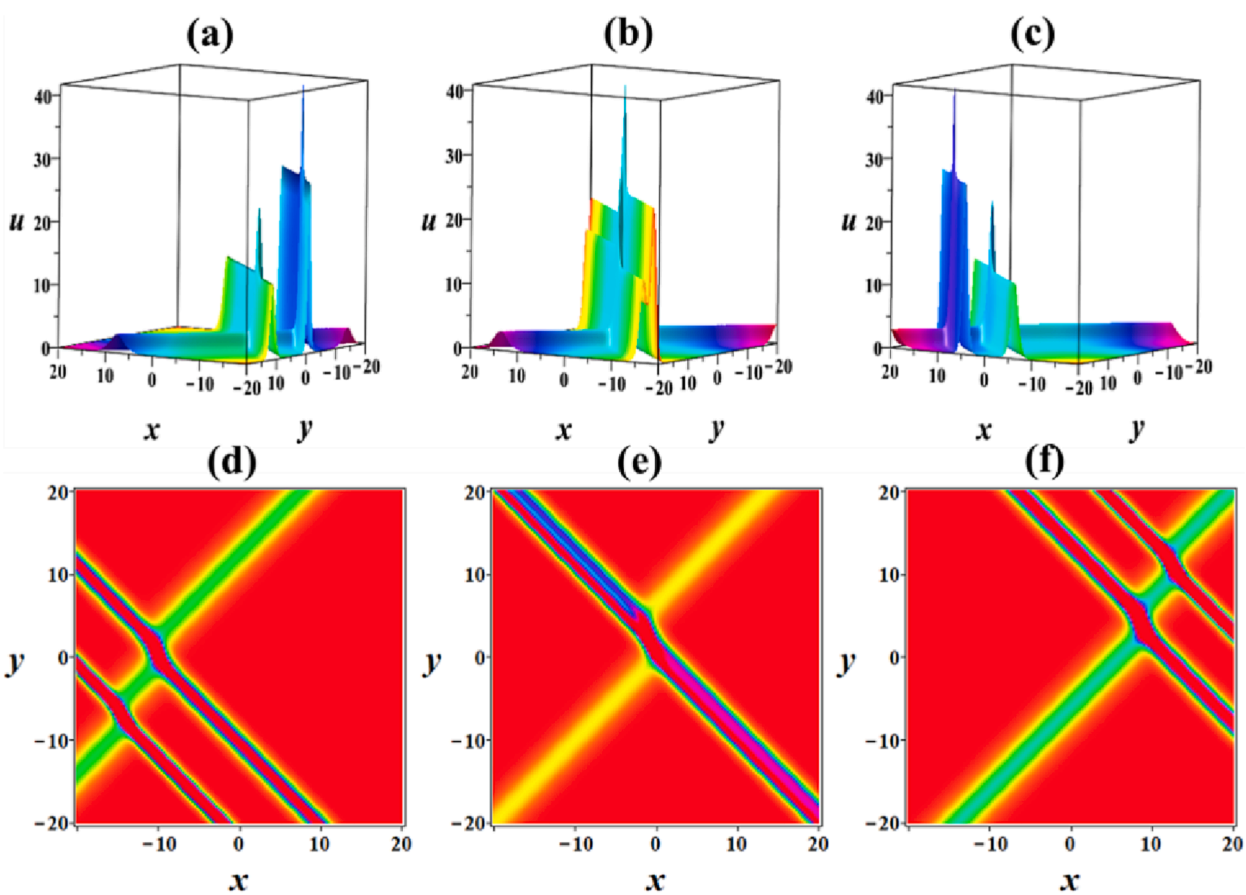

Fig. 9. The profile of interaction between two parallel and one-line soliton solutions via Eq. (3.18) in the $(\mathbf{x}, \mathbf{y})$ plane with $r_1 = 3, r_2 = 2, r_3 = -1, s_1 = 3, s_2 = 2, s_3 = 1, \omega_1 = 0, \omega_2 = 0, \omega_3 = 0, \alpha = 1, \gamma = 1, b = 1, d = 1,$ and $e = 1$: 3D plot for (a) $t = -1$, (b) $t = 0$, and (c) $t = 1$. (d)-(f) the corresponding density plot of (a)-(c).

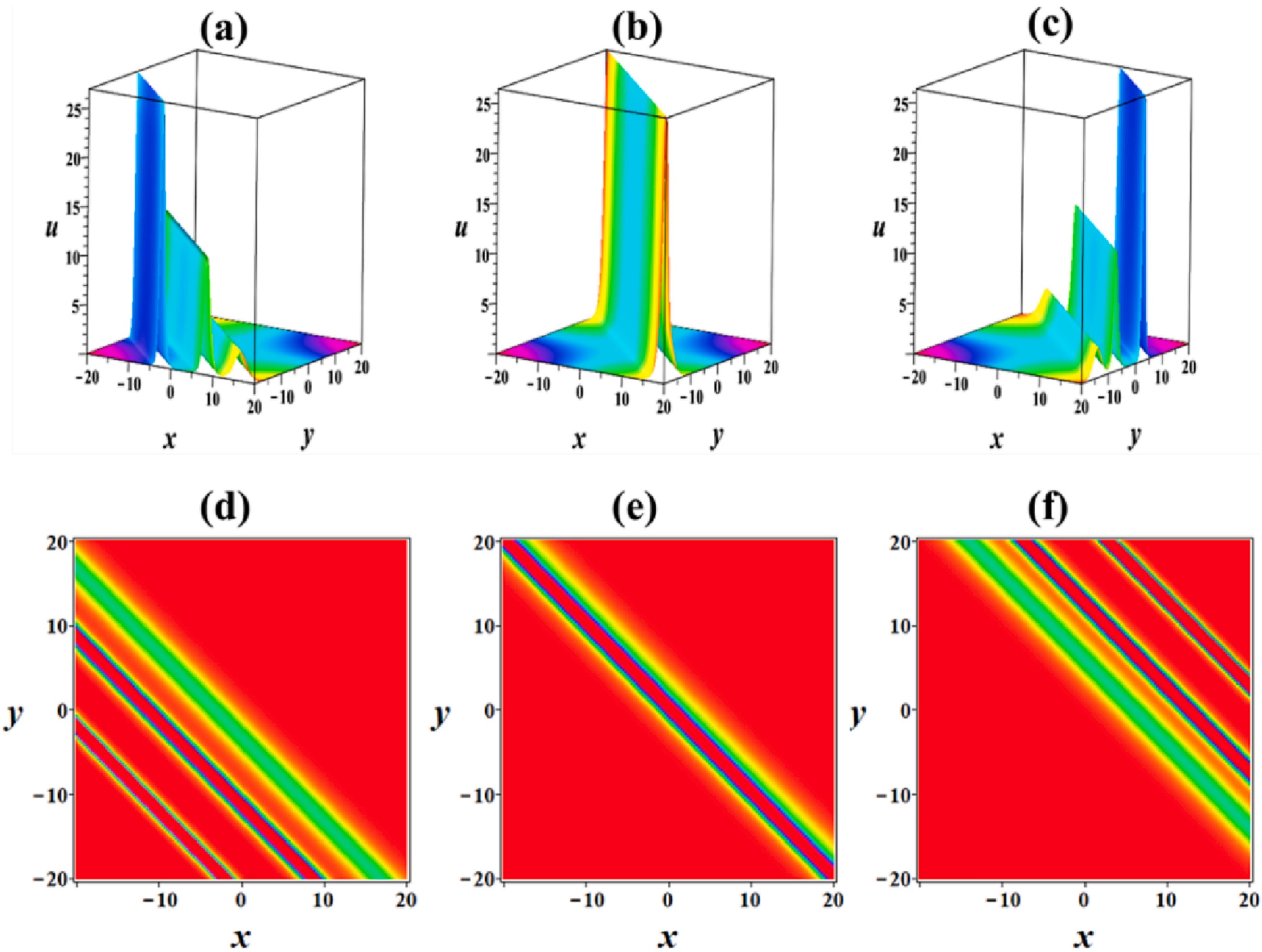

Fig. 10. The profile of three parallel soliton molecules solution via Eq. (3.19) in the $(\mathbf{x},\mathbf{y})$ plane with $r_1=3$, $r_2=1, r_3=2, s_1=3, s_2=1, s_3=2$, $\omega_1=0, \omega_2=0$, $\omega_3=0, \alpha=1, \gamma=1, b=1, d=1$, and $e=1$: 3D plot for (a) $t=-2$, (b) $t=0$, and (c) $t=2$. (d)-(f) the corresponding density plot of (a)-(c).

Here, the obtained solution of Eq. (3.19) is shown by the 3D and density plots, which is presented in Fig. 10**(a)-(f)** with various time at $t=-2, t=0, t=2$. In addition, the Fig. 10**(d)-(f)** display the density plot of Fig. 10**(a)-(c)**. Fig. 10 **(e)**, three parallel soliton molecules express one line soliton when at time $t=0$. Moreover, with varying times ($t=-2$ and $t=2$), the shape and amplitude of the three parallel soliton molecules keep unchanged but their position changed.

Family-II: Interaction between one LS and one PB solution

To obtain the interaction of one LS and one PB solution for Eq. (1.2), the parameters p_i, q_i, and ω_i must meet the following requirements for Eq. (3.15) into Eq. (3.14):

$$p_1=l_1+Im_1,\ p_2=l_1-Im_1,\ q_1=r_1+Is_1,\ q_2=r_1-Is_1,\ p_3=l_2,\ q_3=r_2,\ and\ \omega_1=\omega_2=\omega_3=0, \tag{3.20}$$

where $l_1\neq0$, $l_2\neq0$, $m_1\neq0$, $r_1\neq0$, $r_2\neq0$, and $s_1\neq0$.

(i) To obtain the interaction of one LS and one (x,y)-PB solution, which is contained the following conditions $l_1r_2-l_2r_1\neq0$. In Fig. 11 **(a_1)-(a_3),** a density plot is used to show the interaction of one LS with one (x,y)-PB solution. It can be seen from the mentioned figures, their shape and amplitude are the same but their position is changed with varying time at $t=-2, t=0, t=2$.

(ii) To determine the interaction of one LS and one x-PB solution, which contains the conditions $l_1=0, s_1=0$. If taking $m_1=\frac{1}{2}, l_2=-2$, $r_1=1, r_2=2, \omega_1=0, \omega_2=0, \omega_3=0, \alpha=1, \gamma=1, b=1, d=1, e=1$ in (3.20) along with Eq. (3.15), then we can be seen that the interaction of one LS and one x-PB solution are depicted in Fig. 11 **(b_1)-(b_3).**

(iii) Furthermore, if we put $m_1=0$, $r_1=0$ in Eq. (3.20) and take $l_1=\frac{1}{2}, l_2=-1$, $s_1=-1, s_2=3, \omega_1=0, \omega_2=0, \omega_3=0, \alpha=1, \gamma=1, b=1, d=1, e=1$ in Eq. (3.15), then we can get the interaction of one LS and one y-PB solution. Additionally, with varying time ($t=-2, t=0$, $t=2$), obtained solutions are illustrated by a density plot which is displayed in Fig. 11**(c_1)-(c_3)**. On the other hand, for the parallel one LS and one $(x,\ y)$-PB wave, it is maintained the following structure $l_1r_2-l_2r_1=0$. Due to space consumption, the graphical figures are not attached here.

Family-III: Interaction between one lump soliton and one LS solution

To determine the interaction between one lump and one LS for Eq. (1.2), the parameters p_i, q_i, and ω_i must meet the following requirements for Eq. (3.15) into Eq. (3.14):

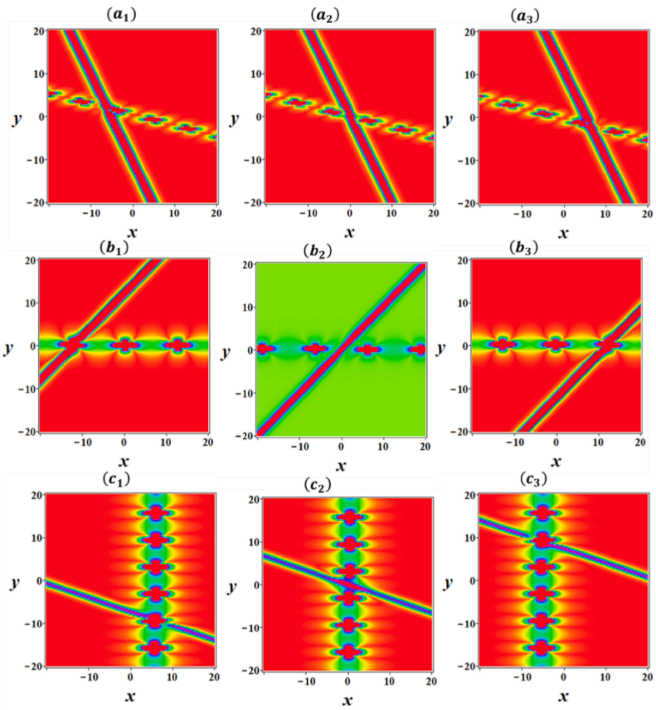

Fig. 11. The profile of interaction between one line soliton and one periodic breather solution $|u(x,y,t)|$ via Eq. (3.15) in the (x,y) plane. (a_1)-(a_3) interaction of one line and one (x,y)-periodic breathers with $l_1=\frac{1}{2}, l_2=2, m_1=-\frac{1}{2}, r_1=2, r_2=1, s_1=1, \omega_1=0, \omega_2=0, \omega_3=0, \alpha=1, \gamma=1, b=1, d=1, e=1$, when $t=-2, t=0, t=2$; (b_1)-(b_3) interaction of one line and one x-periodic breather with $m_1=\frac{1}{2}, l_2=-2, r_1=1, r_2=2, \omega_1=0, \omega_2=0, \omega_3=0, \alpha=1, \gamma=1, b=1, d=1, e=1$, when $t=-2, t=0, t=2$; (c_1)-(c_3) interaction of one line and one y-periodic breather with $l_1=\frac{1}{2}, l_2=-1, s_1=-1, r_2=3, \omega_1=0, \omega_2=0, \omega_3=0, \alpha=1, \gamma=1, b=1, d=1, e=1$, when $t=-2, t=0, t=2$.

$$q_1=m_1p_1, q_2=m_2p_2, q_3=m_3p_3, p_1=l_1\varepsilon, p_2=l_2\varepsilon, \omega_1=\omega_2^*=\pi i, \text{and}\ \omega_3=0. \tag{3.21}$$

Putting Eq. (3.21) in Eq. (3.15) then the function f_3 can be written as

$$f_3=(a_{12}+V_1V_2)l_1l_2\varepsilon^2+(V_1V_2+a_{23}V_1+a_{13}V_2+a_{12}+a_{12}a_{23})e^{\theta_3}l_1l_2\varepsilon^2+O(\varepsilon^3). \tag{3.22}$$

Taking the limit as $\varepsilon\to0$ in Eq. (3.22), then the interaction between one lump and one LS solution of Eq. (1.2) can be written from Eq. (3.15):

$$u=\frac{12\gamma}{\alpha}\left(\ln((a_{12}+V_1V_2)+(V_1V_2+a_{23}V_1+a_{13}V_2+a_{12}+a_{12}a_{23})e^{v_3}\,)\right)_{xx}, \tag{3.23}$$

where

$$V_i=x+m_iy-\left(e+m_i{}^2d+\gamma\right)t, i=1,2, \tag{3.24}$$

$$a_{12}=-d(m_1-m_2)^2, \tag{3.25}$$

$a_{i3}=3\gamma p_3^4-dm_3^2p_3^2+2dp_3^2m_im_3-dp_3^2m_i^2, i=1,2,$ (3.26) and

$$v_3=p_3x+p_3m_3y-\frac{(\gamma p_3^4+dm_3^2p_3^2+ep_3^2)t}{p_3}. \tag{3.27}$$

Substituting $l_1=\frac{1}{2}, l_2=2, p_3=-1, r_1=-\frac{1}{4}, s_1=-4, m_3=-\frac{1}{4}, \omega_1=\omega_2^*=I\pi, \omega_3=0, \alpha=1, \gamma=1, b=1, d=1, e=1$ in Eq. (3.23) into Eq. (3.27), we get interaction between one lump and one LS solution. Moreover, the obtained solution of Eq. (3.23) is shown by the 3D and density plot, which is presented in Fig. 12**(a)-(f)** with various time at $t=-0.5, t=0, t=0.5$. In addition, the Fig. 12**(d)-(f)** display the density plot of Fig. 12**(a)-(c)**. Fig. 12**(a)**, the lump soliton first shows on the positive side of the x-axis at time $t=-0.5$, when it separates from the LS. It is also seen from Fig. 12 **(b),** the lump soliton and LS are overlapped when $t=0$. Moreover, at time $t=0.5$, the LS and lump soliton are separated in the opposite positive direction of x-axis, which can observe in Fig. 12 **(c).** However, we deeply investigated that the interaction of lump soliton and LS changes their position but the shape is unchanged. Table 2 provides some mathematical aspects for selecting the proper parameters to produce localized waves and interaction solutions with three-soliton solutions of Eq. (1.2).

Localized wave solutions between four solitons

In this part, we obtain the localized waves and their interaction solutions among four solitons and their explanation of graphs shown by the KSE. The specific localized waves and interaction solutions, viz. two LS and one PB, two PB, one lump and one PB, and two lump soliton solutions. Putting $N=4$ in Eq. (2.7), then the function f_4 can be written as:

$$\begin{aligned}f_4=&1+e^{v_1}+e^{v_2}+e^{v_3}+e^{v_4}+A_{12}e^{v_1+v_2}+A_{13}e^{v_1+v_3}+A_{14}e^{v_1+v_4}+A_{23}e^{v_2+v_3}\\&++A_{24}e^{v_2+v_4}+A_{34}e^{v_3+v_4}+A_{123}e^{v_1+v_2+v_3}+A_{124}e^{v_1+v_2+v_4}+A_{134}e^{v_1+v_3+v_4}\\&+A_{234}e^{v_2+v_3+v_4}+A_{1234}e^{v_1+v_2+v_3+v_4},\end{aligned} \tag{3.28}$$

where the phase shift contains $A_{123}=A_{12}A_{23}A_{13}$ and $A_{1234}=A_{12}A_{13}A_{14}A_{23}A_{24}A_{34}$.

Now, setting Eq. (3.28) into Eq. (2.10) then the four soliton solutions can be written as

$$u=\frac{12\gamma}{\alpha}(\ln f_4)_{xx}, \tag{3.29}$$

Family-I: Interaction between two LS and one PB solutions

If we take $p_1=p_2^*=l_1+Im_1$, $q_1=q_2^*=r_1+Is_1$, $p_3=l_2$, $p_4=l_3$, $q_3=s_2$, $q_4=s_3$, and $\omega_1=\omega_2=\omega_3=\omega_4=0$ in Eq. (3.29), then we can obtain the intersection between two LS and one PB solution from four solitons. For particular values $l_1, l_2, l_3, m_1, r_1, s_1, s_2$, and s_3, the intersection between two LS and one PB can be changed their direction which may be a direction along the (x,y)-axis, x-axis, and y-axis. These directions are as follows:

(i) If substituting the parameters $l_1=\frac{1}{2}, l_2=3, l_3=1, m_1=0, r_1=\frac{1}{6}, s_1=1, s_2=3, s_3=1, \omega_1=0, \omega_2=0, \omega_3=0, \omega_4=0, \alpha=1, \gamma=1, b=1, d=1, e=1$ in Eq. (3.29), then the acquired solution of interaction between two LS and one PB are presented by 3D and density plots in Fig. 13**(a)** and Fig. 13**(d).**

(ii) If setting $l_1=0, m_1=1, l_2=2, l_3=1, r_1=-1, s_1=0, s_2=-5, s_3=2, \omega_1=0, \omega_2=0, \omega_3=0, \omega_4=0, \alpha=1, \gamma=1, b=1, d=1, e=1$ in Eq. (3.29), then the obtained solution of interaction between two LS and one x-PB are presented by 3D and density plots in Fig. 13**(e)** and Fig. 13 **(b)**, whereas the Fig. 13**(e)** displays the density plot of Fig. 13**(b).**

(iii) If putting $l_1=\frac{1}{2}, r_1=0, l_2=3, l_3=1, m_1=0, s_1=1, s_2=3, s_3=1, \omega_1=0, \omega_2=0, \omega_3=0, \omega_4=0, \alpha=1, \gamma=1, b=1, d=1, e=1$ in Eq. (3.29), then the obtained solution of interaction between two LS and one y-PB are displayed by density plot and 3D plots in Fig. 13**(c)** and Fig. 13 **(f)**, whereas the Fig. 13**(f)** presents the density plot of Fig. 13**(c).**

Family-II: Interaction between PB solutions

If putting the parameters $l_1=-\frac{1}{2}, l_2=-\frac{1}{2}, s_1=-\frac{1}{3}, s_2=\frac{1}{2}, \omega_1=0, \omega_2=0, \omega_3=0, \omega_4=0, \alpha=1, \gamma=1, b=1, d=1, e=1$ in Eq. (3.29), then the obtained solution of interaction between two parallel x-PB is presented by 3D and density plots in Fig. 14**(a)** and Fig. 14**(d).** Elsewhere, if we set the parameters $l_1=-\frac{1}{3}, l_2=\frac{1}{2}, s_1=-1, s_2=\frac{1}{2}, \omega_1=0, \omega_2=0, \omega_3=0, \omega_4=0, \alpha=1, \gamma=1, b=1, d=1, e=1$ in Eq. (3.29), we get two parallel y-PB solutions. Moreover, the obtained solution of Eq. (3.29) is shown by the 3D and density plots, which is presented in Fig. 14

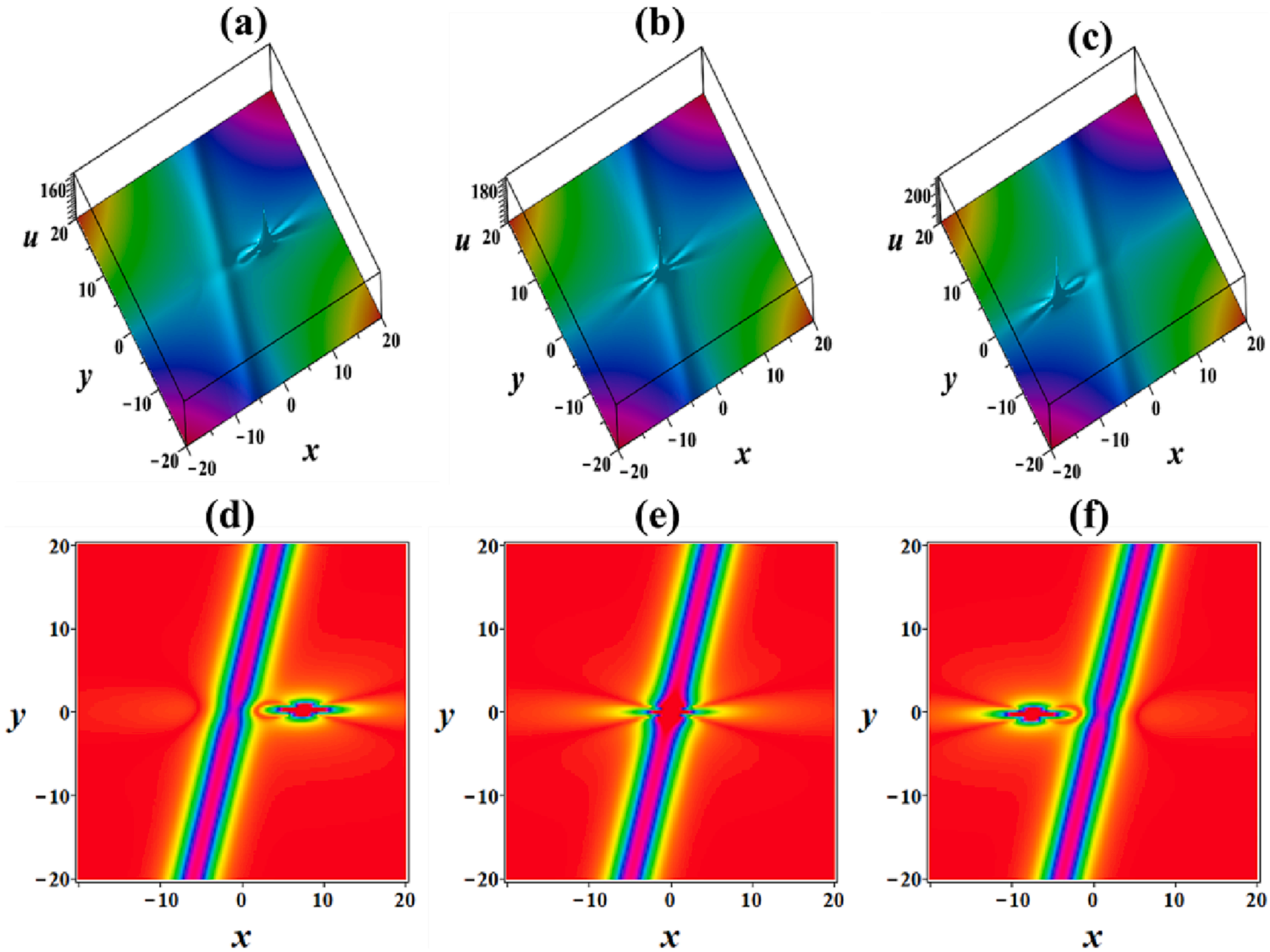

Fig. 12. The profile of one lump and one line soliton solution $|u(x, y, t)|$ via Eq. (3.23) in the $(\mathbf{x}, \mathbf{y})$ plane

(b) and Fig. 14**(e)**. In addition, Fig. 14**(e)** displays the density plot of Fig. 14**(b)**.

Further, considering the parameters $l_1 = \frac{1}{3}, l_2 = \frac{1}{4}, r_1 = \frac{1}{4}, r_2 = -\frac{1}{3}, s_1 = -\frac{1}{2}, s_2 = \frac{1}{2}, \omega_1 = 0, \omega_2 = 0, \omega_3 = 0, \omega_4 = 0, \alpha = 1, \gamma = 1, b = 1, d = 1, e = 1$ in Eq. (3.30), we get interaction between two cross xy-PBs, which is displayed in Fig. 14 **(c)** and Fig. 14 **(f)**. It can be obtained figures that the shape and amplitude remain constant, but their position is changed. However, the propagation process is not shown above all figures for the sake of brevity.

Family-III: Interaction between one lump soliton and one PB solution

To investigate the interaction between one lump soliton and one PB solution for Eq. (1.2), the parameters p_i, q_i, and ω_i must meet the following requirements for Eq. (3.29) into Eq. (3.28):

$$q_i = m_i p_i \; (i = 1, 2, 3, 4),\; p_1 = l_1 \varepsilon,\; p_2 = l_2 \varepsilon,\; \omega_1 = \omega_2^* = \pi I,\; \text{and } \omega_3 = \omega_4 = 0. \tag{3.30}$$

Now, putting Eq. (3.30) in Eq. (2.7) then the function f_4 can be written as

$$\begin{aligned} f_4 = {} & (a_{12} + V_1 V_2) l_1 l_2 \varepsilon^2 + (V_1 V_2 + a_{23} V_1 + a_{13} V_2 + a_{12} + a_{13} a_{23}) e^{v_3} l_1 l_2 \varepsilon^2 \\ & + (V_1 V_2 + a_{24} V_1 + a_{14} V_2 + a_{12} + a_{14} a_{24}) e^{v_4} l_1 l_2 \varepsilon^2 \\ & + a_{34} [V_1 V_2 + (a_{23} + a_{24}) V_1 + (a_{13} + a_{14}) V_2 + a_{12} + (a_{13} + a_{14})(a_{23} + a_{24})] \\ & \times e^{(v_3 + v_4)} l_1 l_2 \varepsilon^2 + O(\varepsilon^3). \end{aligned} \tag{3.31}$$

Taking the limit as $\varepsilon \to 0$ in Eq. (3.31), then the obtained lump soliton solution of Eq. (1.2) can be written from Eq. (3.29), as follows:

$$\begin{aligned} u = {} & \frac{12\gamma}{\alpha} \big(ln \big((a_{12} + V_1 V_2) + (V_1 V_2 + a_{23} V_1 + a_{13} V_2 + a_{12} + a_{13} a_{23}) e^{v_3} + (V_1 V_2 + a_{24} V_1 + a_{14} V_2 + a_{12} + a_{14} a_{24}) e^{v_4} + a_{34} [V_1 V_2 + (a_{23} + a_{24}) V_1 \\ & + (a_{13} + a_{14}) V_2 + a_{12} + (a_{13} + a_{14})(a_{23} + a_{24})] \times e^{(v_3 + v_4)} \big) \big)_{xx} \end{aligned} \tag{3.32}$$

Table 2
Various localized wave forms and their interaction between three solitons.

N-soliton	Localized wave forms	Parameters
$N = 3$	Three LS	$p_i = r_i, q_i = s_i, (i = 1, 2, 3)$, and $\omega_1 = \omega_2 = \omega_3 = 0$. For Cross-LS: $\prod_{i\neq j}(r_is_j - r_js_i) \neq 0$; For Parallel-LS: $\sum_{i\neq j}(r_is_j - r_js_i)^2 = 0$; For cross and parallel-LS: $\prod_{i\neq j}(r_is_j - r_js_i) = 0$ and $\sum_{i\neq j}(r_is_j - r_js_i)^2 \neq 0$.
	One LS + one (x, y)-PB	$p_1 = p_2^* = l_1 + Im_1, q_1 = q_2^* = r_1 + Is_1, p_3 = l_2, q_3 = r_2$. For cross-line interaction: $l_1r_2 - l_2r_1 \neq 0$ and For parallel-line interaction: $l_1r_2 - l_2r_1 = 0$.
	One LS + one x-PB	$p_1 = p_2^* = Im_1, q_1 = q_2 = r_1, p_3 = l_2, q_3 = r_2$, and $\omega_1 = \omega_2 = \omega_3 = 0$.
	One LS + one y-PB	$p_1 = p_2 = l_1, q_1 = q_2^* = Is_1, p_3 = l_2, q_3 = r_2$, and $\omega_1 = \omega_2 = \omega_3 = 0$.
	One LS + one lump soliton	$q_1 = m_1p_1, q_2 = m_2p_2, q_3 = m_3p_3, p_1 = l_1\varepsilon, p_2 = l_2\varepsilon, \omega_1 = \omega_2^* = \pi I$, and $\omega_3 = 0$, and $\varepsilon \to 0$.

where,

$$V_i = x + m_iy - \left(e + m_i{}^2d + \gamma\right)t, i = 1, 2, \tag{3.33}$$

$$a_{12} = -d(m_1 - m_2)^2, \tag{3.34}$$

$$u = \frac{12\gamma}{\alpha}(ln(V_1V_2V_3V_4 + a_{34}V_1V_2 + a_{24}V_1V_3 + a_{23}V_1V_4 + a_{14}V_2V_3 + a_{13}V_2V_4 + a_{12}V_3V_4 + a_{12}a_{34} + a_{13}a_{24} + a_{14}a_{23}))_{xx} \tag{3.40}$$

$$a_{ir} = 3\gamma p_r^4 - dm_r^2p_r^2 + 2dp_r^2m_im_r - dp_r^2m_i^2, (i = 1, 2; r = 3, 4) \tag{3.35}$$

$$a_{34} = \frac{4\left(-dl_3^2q_4^2 + 2dl_3^2q_3q_4 - dl_3^2q_3^2\right)l_3^2}{12\gamma l_3^6 - dl_3^2q_4^2 + 2dl_3^2q_3q_4 - dl_3^2q_3^2} \tag{3.36}$$

and

$$v_i = p_ix + p_im_iy - \frac{\left(\gamma p_i^4 + dm_i^2p_i^2 + ep_i^2\right)t}{p_i}, i = 3, 4. \tag{3.37}$$

Considering $m_1 = m_2^* = r_1 + Is_1$, $q_3 = q_4^* = r_2 + Is_2$, and $p_3 = p_4 = l_3$ with the Eqs. (3.37). Then the solution of Eq. (3.32) indicates the interaction between one lump and one PB. If taking $l_1 = \frac{1}{2}, l_2 = 4, l_3 = \frac{1}{2}, r_1 = 2, r_2 = \frac{1}{2}, s_1 = -4, s_2 = -\frac{1}{2}, \omega_1 = \omega_2^* = I\pi, \omega_3 = 0, \omega_4 = 0, \alpha = 1, \gamma = 1, b = 1, d = 1, e = 1$, then the obtained solution of Eq. (3.32) is shown by the 3D and density plots, which is presented in Fig. 15**(a)-(f)** with various time at $t = -1, t = 0, t = 1$. In addition, Fig. 15**(d)-(f)** display the density plot that corresponds to Fig. 15**(a)-(c)**. At time $t = -1$, the lump solution is located near the breather from the right sides, but when $t = 1$, it is situated opposite of the breather. In addition, it can be observed that one lump and one breather is overlapped at. $t = 0$

Family-IV: Interaction between two lump soliton solutions

To obtain the interaction between two lump soliton solutions for Eq. (1.2), the parameters p_i, q_i, and ω_i must meet the following requirements for Eq. (3.29) into Eq. (3.28):

$$q_i = m_ip_i\ (i = 1,\ 2,\ 3,\ 4),\ p_i = l_i\varepsilon,\ (i = 1,\ 2,\ 3,\ 4),\ \omega_1 = \omega_2^* = \pi I,\ \ and\ \omega_3 = \omega_4^* = \pi i. \tag{3.38}$$

Substituting Eq. (3.38) in Eq. (2.7) then the function f_4 can be written as

$$f_4 = (V_1V_2V_3V_4 + a_{34}V_1V_2 + a_{24}V_1V_3 + a_{23}V_1V_4 + a_{14}V_2V_3 + a_{13}V_2V_4 + a_{12}V_3V_4 + a_{12}a_{34} + a_{13}a_{24} + a_{14}a_{23})l_1l_2l_3l_4\varepsilon^4 + O\left(\varepsilon^5\right). \tag{3.39}$$

Taking the limit as $\varepsilon \to 0$ in Eq. (3.39), then the interaction between two lump soliton solutions of Eq. (1.2) can be written as

where,

$$V_i = x + m_iy - \left(e + m_i{}^2d + \gamma\right)t, i = 1, 2, 3, 4 \tag{3.41}$$

$$a_{ij} = -d(m_1 - m_2)^2, (1 \le i \le j \le 4) \tag{3.42}$$

Considering $m_1 = m_2^* = r_1 + Is_1$, $m_3 = m_4^* = r_2 + Is_2$, and $p_3 = p_4 = l_3$ with the Eqs. (3.42)-(3.41), then the solution of Eq. (3.40) indicates the interaction between the two lump soliton solutions. If taking $l_1 = \frac{1}{3}, l_2 = 1, l_3 = -1, l_4 = 2, r_1 = \frac{1}{5}, r_2 = -3, s_1 = 4, s_2 = 4, \omega_1 = \omega_2^* = I\pi, \omega_3 = \omega_4^* = I\pi, \alpha = 1, \gamma = 1, b = 1, d = 1, e = 1$, then the obtained solution of two lump soliton is presented by the 3D plot in Fig. 16**(a)-(e)**. From Fig. 16, two lump soliton propagates along the y-axis and x-axis direction when $t = -2, t = -1, t = 0, t = 1, t = 2$, respectively. In addition, during that time $(t = -2, t = 2)$, we observed that two lump among this one is visual and another clearly along the x-axis and y-axis direction. It is also seen from the above figures that during the propagation, two lump solitons move closer when the time $(t = 0)$ and otherwise, it separates. Table 3 provides some mathematical aspects for selecting the proper parameters to produce localized waves and interaction solutions with four-soliton solutions of Eq. (1.2).

Discussion and concluding remarks

It is earlier noted that the nonautonomous lump wave, periodic, breather, rogue wave, and resonant multiple soliton solutions to the (3 + 1)-dimensional KS equation, which has been published by particular researchers [2,43,45–55] with variety methods. In this paper, we have chosen a dimensionally reduced (2 + 1)-dimensional KS equation, which leads to N-solitons with each other via the HBM. Thereafter, we have examined the novel interaction and localized wave solutions from N-solitons. According to the authors, there is no study of localized waves and the various interactions of soliton solutions.

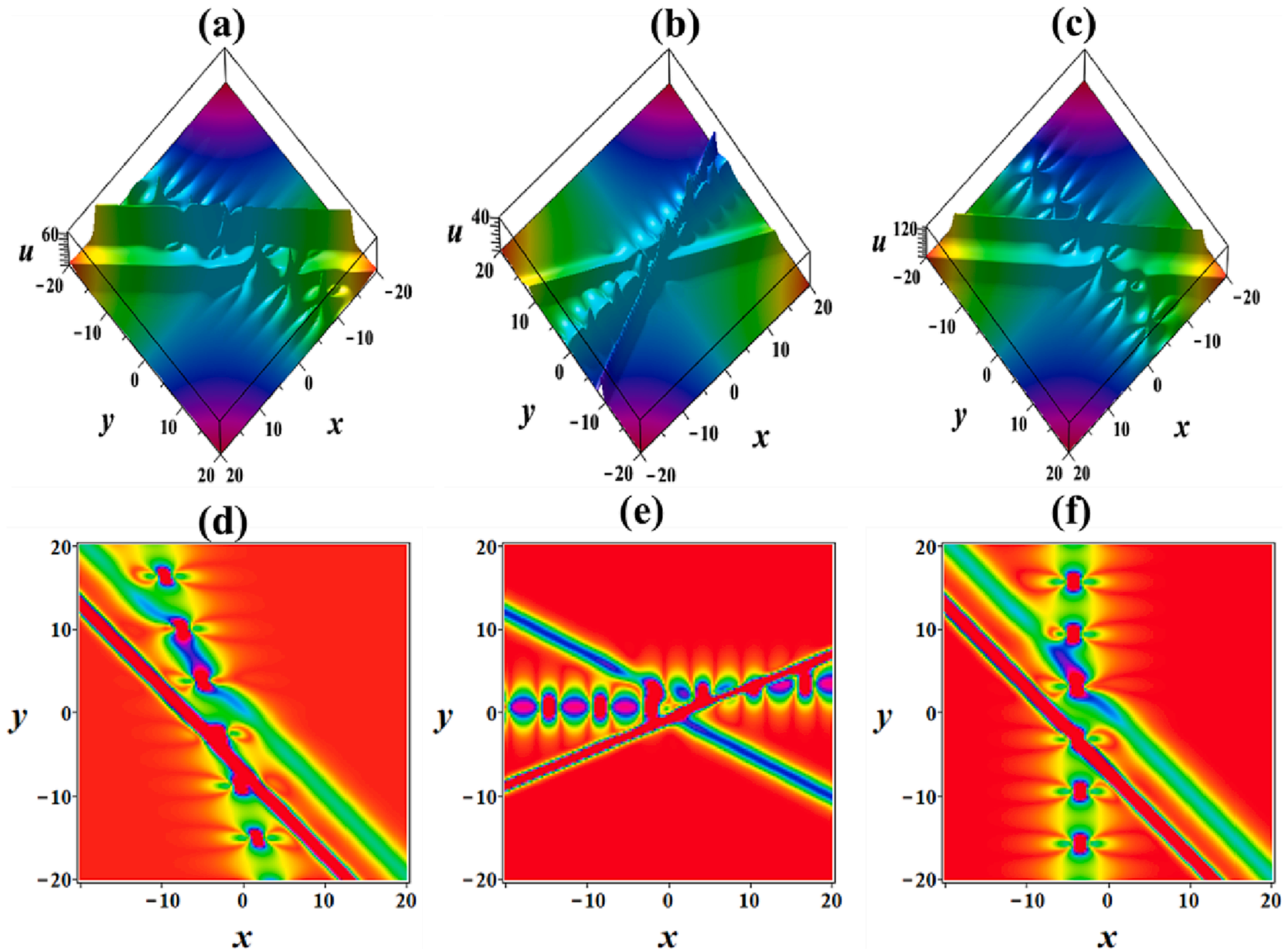

Fig. 13. The profile of interaction between two-line and one-periodic breather solutions $|u(x,y,t)|$ via Eq. (3.29) with $\omega_1 = 0, \omega_2 = 0, \omega_3 = 0, \omega_4 = 0, \alpha = 1, \gamma = 1, b = 1, d = 1, e = 1$ at $t = 1$. (a) two line soliton and one **xy**-periodic breather with $l_1 = \frac{1}{2}, l_2 = 3, l_3 = 1, m_1 = 0, r_1 = \frac{1}{6}, s_1 = 1, s_2 = 3, s_3 = 1$; (b) two line soliton and one **x**-periodic breather with $l_1 = 0, m_1 = 1, l_2 = 2, l_3 = 1, r_1 = -1, s_1 = 0, s_2 = -5, s_3 = 2$; (c) two line soliton and one **y**-periodic breather with $l_1 = \frac{1}{2}, l_2 = 3, l_3 = 1, s_1 = 1, s_2 = 3, s_3 = 1$. (d)-(f) the corresponding density plot of (a)-(c).

To show the importance of localized waves and how they interact with N-soliton solutions in a reduced $(2+1)$-dimensional KS equation, we used Maple 17 software to display 3D and density plots to obtain solutions, which represents soliton, breather, rogue, lump, and their various interaction solutions. A variety of interaction solutions can happen between various wave patterns such as one LS and one PB, one LS and one lump soliton, two LS and one PB, two PBs, and two lump solitons. In Fig. 1, we display the N-soliton solutions of Eq. (1.2) as determined by Eq. (2.10). It is clear from Fig. 1 that interaction between N-soliton solutions is entirely elastic. For $N = 2$, the cross-LS, parallel-LS, one y-PB, one (x, y)-PB, one x-PB, lump soliton, and rogue wave solutions are determined, which are displayed in Figs. 2-7. In addition, for $N = 3$, we have investigated the various interaction solutions from three solitons, such as three cross-LS, two parallel-LS and one LS, three parallel-LS, one LS, and one PB for (x, y), one LS and one x-PB, one LS and one y-PB, and one lump and one LS through the selection of specific parameters, as depicted in Figs. 8-12. Finally, for $N = 4$, we also presented a variety of interaction solutions from four solitons, for example, two LS and xy-PB, two LS and one x-PB, two LS and one y-PB, two parallel x-PB, two parallel y-PB, two cross xy-PB, one lump and one PB, and two lump solitons, which are displayed in Figs. 13-16. It is significant to note that the parameters for the long wave limit approach, which is used to calculate the lump soliton and rogue waves, are constrained [59]. Tables 1-3 present mathematical criteria for ensuring the stability of localized wave and their interaction solutions derived from two, three, and four soliton solutions of Eq. (1.2). These tables provide guidelines for selecting appropriate constraint parameters. It should be noted that the article does not provide interaction solutions for $N \geq 5$, because the computer used to analyze the data cannot handle such complex calculations. Moreover, in the future, we will focus on interaction solutions of higher order N-soliton and consider how to provide these interactions with some better parameters. The findings of this study may be helpful for explaining the propagation of nonlinear waves in a bubbly liquid.

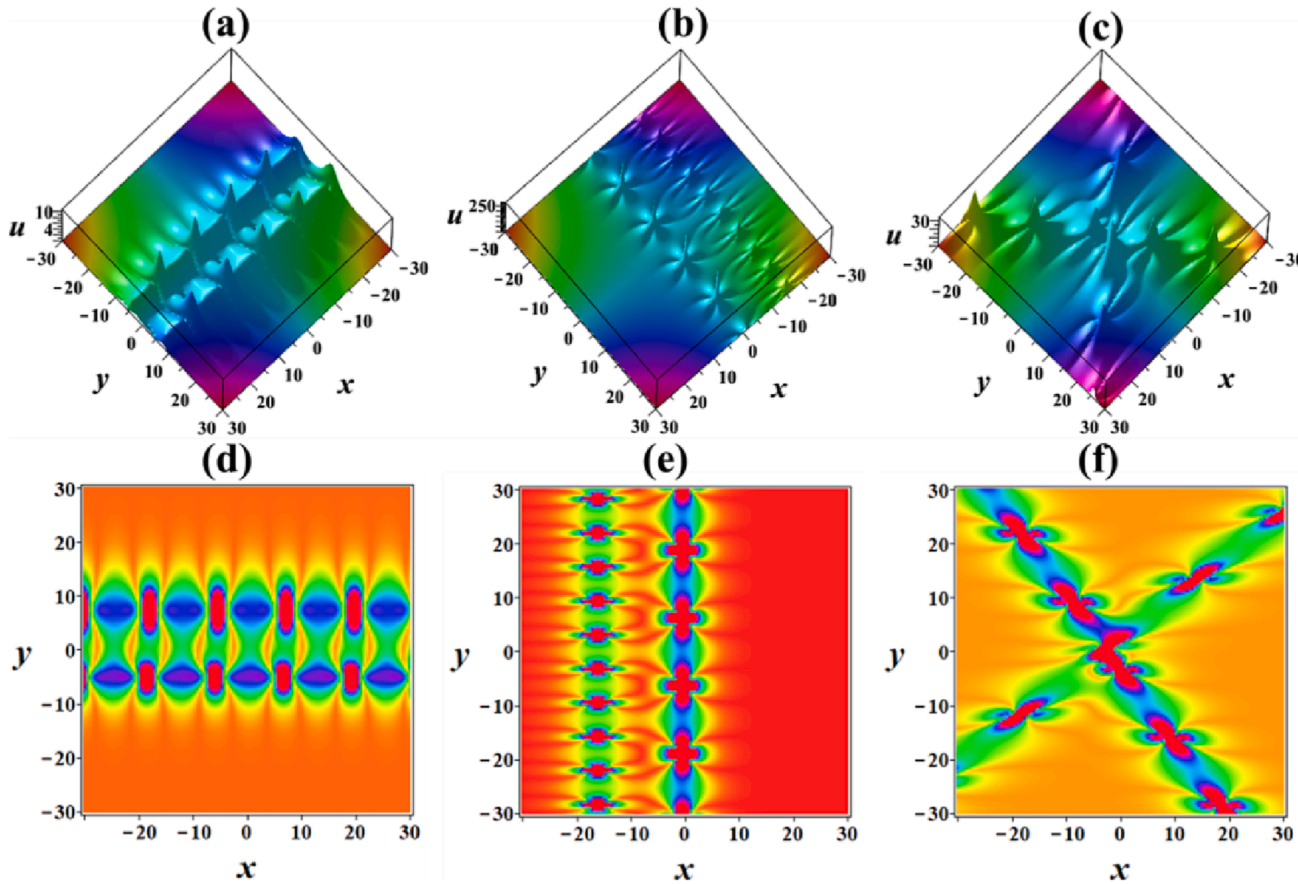

Fig. 14. The profile of the interaction between two periodic breather solutions via Eq. (3.29) with $\omega_1 = 0, \omega_2 = 0, \omega_3 = 0, \omega_4 = 0, \alpha = 1, \gamma = 1, b = 1, d = 1, e = 1$ at $t = 1$. (a) two parallel **x**-periodic breathers with $l_1 = -\frac{1}{2}, l_2 = -\frac{1}{2}, s_1 = -\frac{1}{3}, s_2 = \frac{1}{2}$; (b) two parallel **y**-periodic breathers with $l_1 = -\frac{1}{3}, l_2 = \frac{1}{2}, s_1 = -1, s_2 = \frac{1}{2}$; (c) two cross **xy**-periodic breathers with $l_1 = \frac{1}{3}, l_2 = \frac{1}{4}, r_1 = \frac{1}{4}, r_2 = -\frac{1}{3}, s_1 = -\frac{1}{2}, s_2 = \frac{1}{2}$. (d)-(f) the corresponding density plot of (a)-(c).

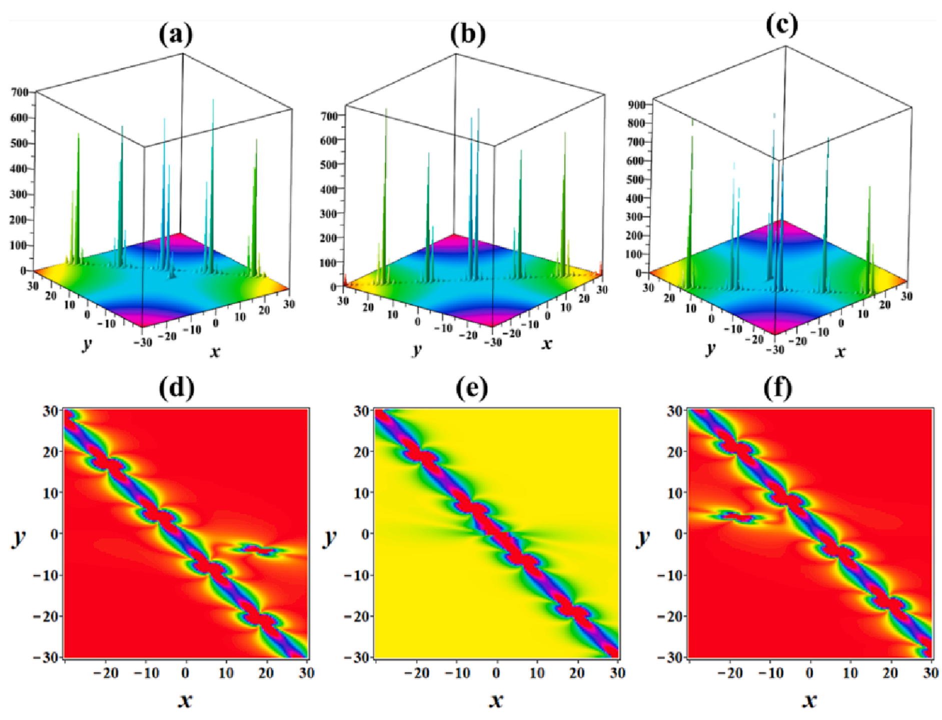

Fig. 15. The profile of interaction solutions between one lump and one periodic breather $|u(x, y, t)|$ via Eq. (3.32) in the $(\mathbf{x}, \mathbf{y})$ plane with $l_1 = 1, l_2 = 4, l_3 = \frac{1}{2}$, $r_1 = 2, r_2 = \frac{1}{2}, s_1 = 5, s_2 = 5, \omega_1 = \omega_2^* = I\pi, \omega_3 = 0, \omega_4 = 0, \alpha = 1, \gamma = 1, b = 1, d = 1, e = 1$. 3D plot for (a) $t = -0.25$, (b) $t = 0$, and (c) $t = 0.25$. (d)-(f) the corresponding density plot of (a)-(c).

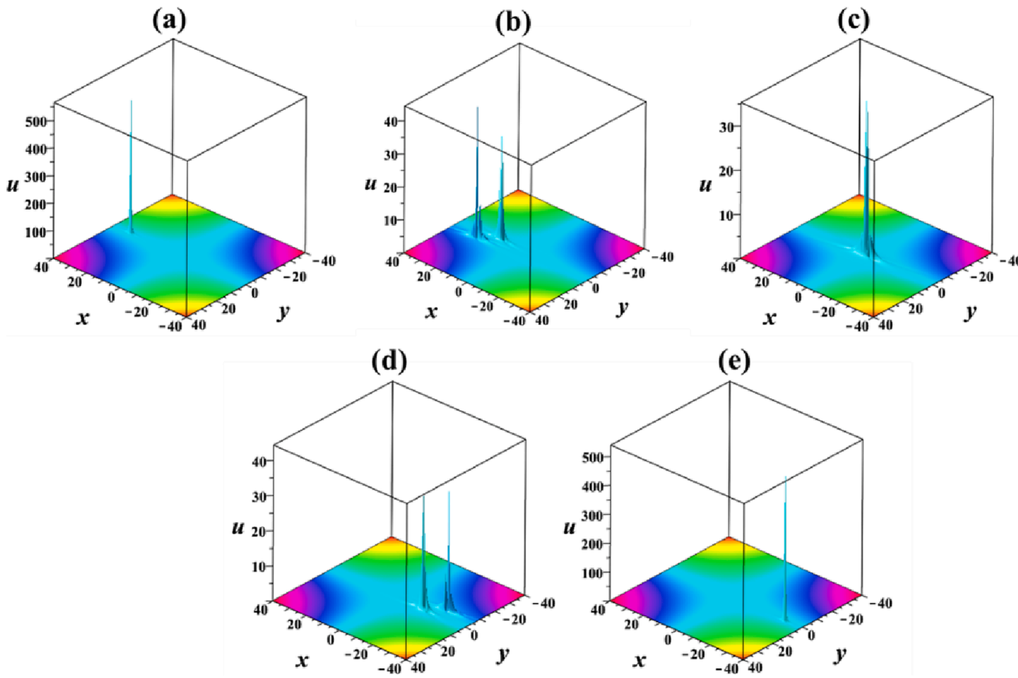

Fig. 16. The profile of interaction solution between two lump soliton solutions $|u(x,y,t)|$ via Eq. (3.40) in the (x,y) plane with $l_1 = \frac{1}{3}, l_2 = 1, l_3 = -1, l_4 = 2$, $r_1 = \frac{1}{5}, r_2 = -3, s_1 = 4, s_2 = 4, \omega_1 = \omega_2^* = I\pi, \omega_3 = 0, \omega_4 = 0, \alpha = 1, \gamma = 1, b = 1, d = 1, e = 1$. 3D plot for (a) $t = -2$, (b) $t = -1$, (c) $t = 0$, and (d)$t = 1$, (e)$t = 2$.

Table 3
Various localized wave forms and their interaction between four solitons.

N-soliton	Localized wave forms	Parameters
$N = 4$	Two LS and one *xy*-PB	$p_1 = p_2 = l_1, q_1 = q_2^* = r_1 + Is_1, p_3 = l_2, p_4 = l_3, q_3 = s_2, q_4 = s_3$, and $\omega_1 = \omega_2 = \omega_3 = \omega_4 = 0$.
	Two LS and one *x*-PB	$p_1 = p_2^* = Im_1, q_1 = q_2 = r_1, p_3 = l_2, p_4 = l_3, q_3 = s_2, q_4 = s_3$, and $\omega_1 = \omega_2 = \omega_3 = \omega_4 = 0$.
	Two LS and one *y*-PB	$p_1 = p_2 = l_1, q_1 = q_2^* = Is_1, p_3 = l_2\ p_4 = l_3, q_3 = s_2, q_4 = s_3$, and $\omega_1 = \omega_2 = \omega_3 = \omega_4 = 0$.
	Two parallel *x*-PB	$p_1 = p_2^* = Il_1, q_1 = q_2 = s_1, p_3 = p_4^* = Il_2, q_3 = q_4 = s_2$, and $\omega_1 = \omega_2 = \omega_3 = \omega_4 = 0$.
	Two parallel *y*-PB	$p_1 = p_2 = l_1, q_1 = q_2^* = Is_1, p_3 = p_4 = l_2, q_3 = q_4^* = Is_2$, and $\omega_1 = \omega_2 = \omega_3 = \omega_4 = 0$.
	Two crosses (x,y)-PB	$p_1 = p_2 = l_1, q_1 = q_2^* = r_1 + Is_1, p_3 = p_4 = l_2, q_3 = q_4^* = r_2 + Is_2$, and $\omega_1 = \omega_2 = \omega_3 = \omega_4 = 0$.
	One lump soliton and one PB	$q_1 = m_1 p_1, q_2 = m_2 p_2, p_3 = p_4 = l_3, q_3 = q_4^* = r_2 + Is_2, p_1 = l_1\varepsilon, p_2 = l_2\varepsilon, \omega_1 = \omega_2^* = I\pi, \omega_3 = \omega_4 = 0, m_1 = m_2^* = r_1 + Is_1, \varepsilon \to 0$.
	Two lump solitons	$q_1 = m_1 p_1, q_2 = m_2 p_2, q_3 = m_3 p_3, q_4 = m_4 p_4, p_1 = l_1\varepsilon, p_2 = l_2\varepsilon, p_3 = l_3\varepsilon, p_4 = l_4\varepsilon, \omega_1 = \omega_2^* = \omega_3 = \omega_4^* = I\pi, m_1 = m_2^* = r_1 + Is_1, m_3 = m_4^* = r_2 + Is_2, \varepsilon \to 0$.

CRediT authorship contribution statement

Md. Nuruzzaman: Conceptualization, Methodology, Supervision, Writing – original draft. **Dipankar Kumar:** Writing – original draft, Investigation. **Mustafa Inc:** Writing – review & editing, Conceptualization. **M. Alhaz Uddin:** Formal analysis. **Rubayyi T. Alqahtani:** Funding acquisition.

Declaration of Competing Interest

The authors declare that they have no known competing financial interests or personal relationships that could have appeared to influence the work reported in this paper.

Data availability

No data was used for the research described in the article.

Acknowledgment

The authors extend their appreciation to the Deanship of Scientific Research at Imam Mohammad Ibn Saud Islamic University (IMSIU) for funding and supporting this work through Research Partnership Program no RP-21-09-07.

Funding

This work was supported and funded by the Deanship of Scientific Research at Imam Mohammad Ibn Saud Islamic University (IMSIU) (Grant number IMSIU-RP23032).

References

[1] Singh S, Mukherjee A, Sakkaravarthi K, Murugesan K. Higher dimensional localized and periodic wave dynamics in an integrable (2+1)-dimensional deep water oceanic wave model. Waves Random Complex Media 2023;33(1):78–97.
[2] Yano T, Kanagawa T, Watanabe M, Fujikawa S. Nonlinear wave propagation in bubbly liquids. In: Delale CF, editor. Bubble Dynamics and Shock Waves. Berlin, Heidelberg: Springer Berlin Heidelberg; 2013. p. 107–40.
[3] Li BQ, Ma YL. Optical soliton resonances and soliton molecules for the Lakshmanan–Porsezian–Daniel system in nonlinear optics. Nonlinear Dyn 2023 Apr;111(7):6689–99.
[4] Yang DY, Tian B, Wang M, Zhao X, Shan WR, Jiang Y. Lax pair, Darboux transformation, breathers and rogue waves of N-coupled nonautonomous nonlinear Schrödinger system for an optical fiber or plasma. Nonlinear Dyn 2022 Feb;107(3):2657–66.
[5] Wang C, Fang H. General high-order localized waves to the Bogoyavlenskii–Kadomtsev–Petviashvili equation. Nonlinear Dyn 2020 Mar;100(1):583–99.

[6] Wang H, Zhou Q, Biswas A, Liu W. Localized waves and mixed interaction solutions with dynamical analysis to the Gross-Pitaevskii equation in the Bose-Einstein condensate. Nonlinear Dyn 2021 Sep;106(1):841–54.
[7] Wang L, Zhu Y-J, Wang Z-Q, Xu T, Qi F-H, Xue Y-S. Asymmetric Rogue waves, breather-to-soliton conversion, and nonlinear wave interactions in the Hirota–Maxwell–Bloch system. J Phys Soc Jpn 2016;85(2):024001.
[8] Yue Y, Huang L, Chen Y. N-solitons, breathers, lumps and rogue wave solutions to a (3+1)-dimensional nonlinear evolution equation. Comput Math Appl 2018 Apr 1; 75(7):2538–48.
[9] Li BQ. Loop-like kink breather and its transition phenomena for the Vakhnenko equation arising from high-frequency wave propagation in electromagnetic physics. Appl Math Lett 2021 Feb;1(112):106822.
[10] Ankiewicz A, Akhmediev N. Rogue wave-type solutions of the mKdV equation and their relation to known NLSE rogue wave solutions. Nonlinear Dyn 2018 Feb;91(3): 1931–8.
[11] Ma YL, Li BQ. Bifurcation solitons and breathers for the nonlocal Boussinesq equations. Appl Math Lett 2022 Feb;1(124):107677.
[12] Ma WX. The inverse scattering transform and soliton solutions of a combined modified Korteweg–de Vries equation. J Math Anal Appl 2019 Mar 1;471(1–2): 796–811.
[13] Yin YH, Lü X, Ma WX. Bäcklund transformation, exact solutions and diverse interaction phenomena to a (3+1)-dimensional nonlinear evolution equation. Nonlinear Dyn 2022 Jun;108(4):4181–94.
[14] Kumar D, Seadawy AR, Joardar AK. Modified Kudryashov method via new exact solutions for some conformable fractional differential equations arising in mathematical biology. Chin J Phys 2018 Feb 1;56(1):75–85.
[15] Zhou H, Chen Y. Breathers and rogue waves on the double-periodic background for the reverse-space-time derivative nonlinear Schrödinger equation. Nonlinear Dyn 2021;106(4):3437–51.
[16] Guo HD, Xia TC. Multi-soliton solutions for a higher-order coupled nonlinear Schrödinger system in an optical fiber via Riemann-Hilbert approach. Nonlinear Dyn 2021 Jan;103(2):1805–16.
[17] Liu B, Zhang XE, Wang B, Lü X. Rogue waves based on the coupled nonlinear Schrödinger option pricing model with external potential. Mod Phys Lett B 2022 May 30;36(15):2250057.
[18] Pu JC, Chen Y. Data-driven vector localized waves and parameters discovery for Manakov system using deep learning approach. Chaos Solitons Fractals 2022 Jul;1 (160):112182.
[19] Lü X, Chen S-J. Interaction solutions to nonlinear partial differential equations via Hirota bilinear forms: one-lump-multi-stripe and one-lump-multi-soliton types. Nonlinear Dyn 2021;103(1):947–77.
[20] Kumar D, Joardar AK, Hoque A, Paul GC. Investigation of dynamics of nematicons in liquid crystals by extended sinh-Gordon equation expansion method. Opt Quant Electron 2019 Jul;51(7):1–36.
[21] Kumar D, Manafian J, Hawlader F, Ranjbaran A. New closed form soliton and other solutions of the Kundu-Eckhaus equation via the extended sinh-Gordon equation expansion method. Optik 2018 May;1(160):159–67.
[22] Zhao YW, Xia JW, Lü X. The variable separation solution, fractal and chaos in an extended coupled (2+1)-dimensional Burgers system. Nonlinear Dyn 2022 Jun;108 (4):4195–205.
[23] Kumar D, Hosseini K, Samadani F. The sine-Gordon expansion method to look for the traveling wave solutions of the Tzitzéica type equations in nonlinear optics. Optik 2017 Nov;1(149):439–46.
[24] Chen S-J, Lü X, Yin Y-H. Dynamic behaviors of the lump solutions and mixed solutions to a (2+1)-dimensional nonlinear model. Commun Theor Phys 2023;75 (5):055005.
[25] Kaur L, Wazwaz AM. Painlevé analysis and invariant solutions of generalized fifth-order nonlinear integrable equation. Nonlinear Dyn 2018 Dec;94(4):2469–77.
[26] Kumar D, Paul GC. Solitary and periodic wave solutions to the family of nonlinear conformable fractional Boussinesq-like equations. Mathematical Methods in the Applied Sciences 2021 Mar 15;44(4):3138–58.
[27] Pu JC, Chen Y. Integrability and exact solutions of the (2+1)-dimensional KdV equation with bell polynomials approach. Acta Mathematicae Applicatae Sinica, English Series 2022 Oct;38(4):861–81.
[28] Kumar D, Raju I, Paul GC, Ali ME, Haque MD. Characteristics of lump-kink and their fission-fusion interactions, rogue, and breather wave solutions for a (3+1)-dimensional generalized shallow water equation. Int J Comput Math 2022 Apr 3;99 (4):714–36.
[29] Li BQ, Ma YL. Hybrid soliton and breather waves, solution molecules and breather molecules of a (3+1)-dimensional Geng equation in shallow water waves. Phys Lett A 2023 Mar;5(463):128672.
[30] Kumar D, Park C, Tamanna N, Paul GC, Osman MS. Dynamics of two-mode Sawada-Kotera equation: Mathematical and graphical analysis of its dual-wave solutions. Results Phys 2020 Dec;1(19):103581.
[31] Nuruzzaman M, Kumar D. Lumps with their some interactions and breathers to an integrable (2+1)-dimensional Boussinesq equation in shallow water. Results Phys 2022 May;23:105642.
[32] Liu Y, Wen XY, Wang DS. The N-soliton solution and localized wave interaction solutions of the (2+1)-dimensional generalized Hirota-Satsuma-Ito equation. Comput Math Appl 2019 Feb 15;77(4):947–66.
[33] Ma Y-L, Wazwaz A-M, Li B-Q. New extended Kadomtsev-Petviashvili equation: multiple soliton solutions, breather, lump and interaction solutions. Nonlinear Dyn 2021;104(2):1581–94.
[34] Li BQ, Ma YL. Soliton resonances and soliton molecules of pump wave and Stokes wave for a transient stimulated Raman scattering system in optics. The European Physical Journal Plus 2022 Nov 9;137(11):1227.
[35] Wu J, Liu Y, Piao L, Zhuang J, Wang DS. Nonlinear localized waves resonance and interaction solutions of the (3+1)-dimensional Boiti–Leon–Manna–Pempinelli equation. Nonlinear Dyn 2020 Apr;100(2):1527–41.
[36] Li BQ, Wazwaz AM, Ma YL. Two new types of nonlocal Boussinesq equations in water waves: bright and dark soliton solutions. Chin J Phys 2022 Jun;1(77): 1782–8.
[37] Liu W, Zhang Y. Dynamics of localized waves and interaction solutions for the (3+ 1) dimensional B-type Kadomtsev–Petviashvili–Boussinesq equation. Adv Difference Equations 2020 Dec;2020(1):1–2.
[38] Ma YL, Wazwaz AM, Li BQ. A new (3+1)-dimensional Kadomtsev-Petviashvili equation and its integrability, multiple-solitons, breathers and lump waves. Math Comput Simul 2021 Sep;1(187):505–19.
[39] Kumar D, Nuruzzaman M, Paul GC, Hoque A. Novel localized waves and interaction solutions for a dimensionally reduced (2+1)-dimensional Boussinesq equation from N-soliton solutions. Nonlinear Dyn 2022 Feb;107(3):2717–43.
[40] Ma YL, Wazwaz AM, Li BQ. A new (3+1)-dimensional Sakovich equation in nonlinear wave motion: Painlevé integrability, multiple solitons and soliton molecules. Qualitative Theory of Dynamical Systems 2022 Dec;21(4):1–7.
[41] Ma YL, Wazwaz AM, Li BQ. Novel bifurcation solitons for an extended Kadomtsev-Petviashvili equation in fluids. Phys Lett A 2021 Oct;18(413):127585.
[42] Kudryashov NA, Sinelshchikov DI. Nonlinear waves in bubbly liquids with consideration for viscosity and heat transfer. Phys Lett A 2010 Apr 19;374(19–20): 2011–6.
[43] Tang X, Chen Y. Lumps, breathers, rogue waves and interaction solutions to a (3+ 1)-dimensional Kudryashov-Sinelshchikov equation. Mod Phys Lett B 2020 Apr 30; 34(12):2050117.
[44] Chukkol YB, Mohamad MNB, Muminov M. Explicit solutions to the (3+1)-dimensional Kudryashov-Sinelshchikov equations in bubbly flow dynamics. J Appl Math 2018;2018:1–9.
[45] Feng Y, Bilige S. Resonant multi-soliton and multiple rogue wave solutions of (3+ 1)-dimensional Kudryashov-Sinelshchikov equation. Phys Scr 2021;96(9):095217.
[46] Kuo CK. A study on the resonant multi-soliton waves and the soliton molecule of the (3+1)-dimensional Kudryashov-Sinelshchikov equation. Chaos Solitons Fractals 2021 Nov;1(152):111480.
[47] El-Shiekh RM, Gaballah M, Elelamy AF. Similarity reductions and wave solutions for the 3D-Kudryashov–Sinelshchikov equation with variable-coefficients in gas bubbles for a liquid. Results Phys 2022 Sep;1(40):105782.
[48] Cr J, Dubey RK, Benton D, A R. The exact solutions for Kudryashov and Sinelshchikov equation with variable coefficients. Phys Scr 2022;97(9):095212.
[49] Hu Z, Wang F, Zhao Y, Lan Z, Li M. Nonautonomous lump waves of a (3+1)-dimensional Kudryashov-Sinelshchikov equation with variable coefficients in bubbly liquids. Nonlinear Dyn 2021 Jun;104(4):4367–78.
[50] Yang H, Liu W, Yang B, He B. Lie symmetry analysis and exact explicit solutions of three-dimensional Kudryashov-Sinelshchikov equation. Commun Nonlinear Sci Numer Simul 2015 Oct 1;27(1–3):271–80.
[51] Inc M, Aliyu AI, Yusuf A, Baleanu D. New solitary wave solutions and conservation laws to the Kudryashov-Sinelshchikov equation. Optik 2017 Aug;1(142):665–73.
[52] Rehman HU, Ullah N, Imran MA. Exact solutions of Kudryashov-Sinelshchikov equation using two analytical techniques. The European Physical Journal Plus 2021 Jun;136(6):1–3.
[53] Seadawy AR, Iqbal M, Lu D. Nonlinear wave solutions of the Kudryashov-Sinelshchikov dynamical equation in mixtures liquid-gas bubbles under the consideration of heat transfer and viscosity. Journal of Taibah University for Science 2019 Dec 11;13(1):1060–72.
[54] Akram G, Sadaf M, Dawood M. Kink, periodic, dark and bright soliton solutions of Kudryashov-Sinelshchikov equation using the improved tanφη2-expansion technique. Opt Quant Electron 2021 Aug;53(8):1–25.
[55] Liu X. Bifurcation and the exact smooth, cusp solitary and periodic wave solutions of the generalized Kudryashov-Sinelshchikov equation. Ricerche mat 2021 Nov;70 (2):461–77.
[56] Zakharov VE, Faddeev LD. Korteweg–de Vries equation: a completely integrable Hamiltonian system. Funktsional'nyi Analiz i ego Prilozheniya 1971;5(4):18–27.
[57] Wang XB, Tian SF, Yan H, Zhang TT. On the solitary waves, breather waves and rogue waves to a generalized (3+1)-dimensional Kadomtsev-Petviashvili equation. Comput Math Appl 2017 Aug 1;74(3):556–63.
[58] Yue Y, Chen Y. Dynamics of localized waves in a (3+1)-dimensional nonlinear evolution equation. Mod Phys Lett B 2019;33(09):1950101.
[59] Ablowitz MJ, Satsuma J. Solitons and rational solutions of nonlinear evolution equations. Journal of Mathematical Physics. 1978 Oct; 19(10): 2180-6.